OPEN ACCESS

African Journal of Microbiology Research

September 2023
ISSN 1996-0808

DOI: 10.5897/AJMR
www.academicjournals.org

ACADEMIC JOURNALS
expand your knowledge

About AJMR

The African Journal of Microbiology Research (AJMR) is a peer reviewed open access journal. The journal commenced publication in May 2007. The journal covers all areas of microbiology such as environmental microbiology, clinical microbiology, immunology, virology, bacteriology, phycology, molecular and cellular biology, molecular microbiology, food microbiology, mycology and parasitology, microbial ecology, probiotics and prebiotics and industrial microbiology.

Indexing

CAB Abstracts, CABI's Global Health Database, Chemical Abstracts (CAS Source Index) Dimensions Database, Google Scholar, Matrix of Information for The Analysis of Journals (MIAR), Microsoft Academic, Research Gate

Open Access Policy

Open Access is a publication model that enables the dissemination of research articles to the global community without restriction through the internet. All articles published under open access can be accessed by anyone with internet connection.

The African Journal of Microbiology Research is an Open Access journal. Abstracts and full texts of all articles published in this journal are freely accessible to everyone immediately after publication without any form of restriction.

Article License

All articles published by African Journal of Microbiology Research are licensed under the Creative Commons Attribution 4.0 International License. This permits anyone to copy, redistribute, remix, transmit and adapt the work provided the original work and source is appropriately cited. Citation should include the article DOI. The article license is displayed on the abstract page the following statement:

This article is published under the terms of the Creative Commons Attribution License 4.0
Please refer to https://creativecommons.org/licenses/by/4.0/legalcode for details about Creative Commons Attribution License 4.0

Article Copyright

When an article is published by in the African Journal of Microbiology Research, the author(s) of the article retain the copyright of article. Author(s) may republish the article as part of a book or other materials. When reusing a published article, author(s) should; Cite the original source of the publication when reusing the article. i.e. cite that the article was originally published in the African Journal of Microbiology Research. Include the article DOI, Accept that the article remains published by the African Journal of Microbiology Research (except in occasion of a retraction of the article).

The article is licensed under the Creative Commons Attribution 4.0 International License.

A copyright statement is stated in the abstract page of each article. The following statement is an example of a copyright statement on an abstract page.
Copyright ©2016 Author(s) retains the copyright of this article.

Self-Archiving Policy

The African Journal of Microbiology Research is a RoMEO green journal. This permits authors to archive any version of their article they find most suitable, including the published version on their institutional repository and any other suitable website.

Digital Archiving Policy

The African Journal of Microbiology Research is committed to the long-term preservation of its content. All articles published by the journal are preserved by Portico. In addition, the journal encourages authors to archive the published version of their articles on their institutional repositories and as well as other appropriate websites.
https://www.portico.org/publishers/ajournals/

Metadata Harvesting

The African Journal of Microbiology Research encourages metadata harvesting of all its content. The journal fully supports and implement the OAI version 2.0, which comes in a standard XML format. See Harvesting Parameter

Memberships and Standards

Academic Journals strongly supports the Open Access initiative. Abstracts and full texts of all articles published by Academic Journals are freely accessible to everyone immediately after publication.

All articles published by Academic Journals are licensed under the Creative Commons Attribution 4.0 International License (CC BY 4.0). This permits anyone to copy, redistribute, remix, transmit and adapt the work provided the original work and source is appropriately cited.

Crossref is an association of scholarly publishers that developed Digital Object Identification (DOI) system for the unique identification published materials. Academic Journals is a member of Crossref and uses the DOI system. All articles published by Academic Journals are issued DOI.

Similarity Check powered by iThenticate is an initiative started by CrossRef to help its members actively engage in efforts to prevent scholarly and professional plagiarism. Academic Journals is a member of Similarity Check.

CrossRef Cited-by Linking (formerly Forward Linking) is a service that allows you to discover how your publications are being cited and to incorporate that information into your online publication platform. Academic Journals is a member of CrossRef Cited-by.

Academic Journals is a member of the International Digital Publishing Forum (IDPF). The IDPF is the global trade and standards organization dedicated to the development and promotion of electronic publishing and content consumption.

Contact

Editorial Office: ajmr@academicjournals.org

Help Desk: helpdesk@academicjournals.org

Website: http://www.academicjournals.org/journal/AJMR

Submit manuscript online http://ms.academicjournals.org

Academic Journals
73023 Victoria Island, Lagos, Nigeria
ICEA Building, 17th Floor,
Kenyatta Avenue, Nairobi, Kenya.

Editors

Prof. Adriano Gomes da Cruz
University of Campinas (UNICAMP),
Brazil.

Prof. Ashok Kumar
School of Biotechnology
Banaras Hindu UniversityUttar Pradesh,
India.

Dr. Mohd Fuat Abd Razak
Infectious Disease Research Centre,
Institute for Medical Research, Jalan
Pahang, Malaysia.

Dr. Adibe Maxwell Ogochukwu
Department of Clinical Pharmacy and
Pharmacy Management,
University of Nigeria
Nsukka, Nigeria.

Dr. Nadezhda Fursova
Molecular Microbiology,
State Research Center for Applied
Microbiology and Biotechnology,
Russia.

Dr. Mehdi Azami
Parasitology & Mycology Department
Baghaeei Lab.
Isfahan, Iran.

Dr. Franco Mutinelli
Istituto Zooprofilattico Sperimentale delle
Venezie Italy.

Prof. Ebiamadon Andi Brisibe
University of Calabar,
Calabar,
Nigeria.

Prof. Nazime Mercan Dogan
Department of Biology
Faculty of Science and Arts
University Denizli Turkey.

Prof. Long-Liu Lin
Department of Applied Chemistry
National Chiayi University
Chiayi County Taiwan.

Prof. Natasha Potgieter
University of Venda
South Africa.

Dr. Tamer Edirne
Department of Family Medicine
University of Pamukkale
Turkey.

Dr. Kwabena Ofori-Kwakye
Department of Pharmaceutics
Kwame Nkrumah University of Science &
Technology
Kumasi, Ghana.

Dr. Tülin Askun
Department of Biology
Faculty of Sciences & Arts
Balikesir University Turkey.

Dr. James Stefan Rokem
Department of Microbiology & Molecular
Genetics
Institute of Medical Research Israel – Canada
The Hebrew University – Hadassah Medical
School Jerusalem, Israel.

Editors

Dr. Afework Kassu
University of Gondar
Ethiopia.

Dr. Wael Elnaggar
Faculty of Pharmacy
Northern Border University
Rafha Saudi Arabia.

Dr. Maulin Shah
Industrial Waste Water Research Laboratory
Division of Applied & Environmental Microbiology, Enviro Technology Limited
Gujarat, India.

Dr. Ahmed Mohammed
Pathological Analysis Department
Thi-Qar University College of Science
Iraq.

Prof. Naziha Hassanein
Department of Microbiology
Faculty of Science
Ain Shams University
Egypt.

Dr. Shikha Thakur
Department of Microbiology
Sai Institute of Paramedical and Allied Sciences India.

Prof. Pongsak Rattanachaikunsopon
Department of Biological Science,
Ubon Ratchathani University,
Thailand.

Dr. Rafael Lopes e Oliveira
Chemical Engineering,
Amazon State University - Uea,
Brazil.

Dr. Annalisa Serio
Faculty of Bioscience and Technology for Food, Agriculture and Environment,
University of Teramo.
Italy

Dr. Samuel K Ameyaw
Civista Medical Center
USA.

Dr. Mahmoud A. M. Mohammed
Department of Food Hygiene and Control
Faculty of Veterinary Medicine
Mansoura University Egypt.

Dr. Anubrata Ghosal
Department of Biology
MIT - Massachusetts Institute of Technology
USA.

Dr. Bellamkonda Ramesh
Department of Food Technology
Vikrama Simhapuri University
India.

Dr. Sabiha Yusuf Essack
Department of Pharmaceutical Sciences
University of KwaZulu-Natal
South Africa.

Dr. Navneet Rai
Genome Center
University of California Davis USA.

Dr. Iheanyi Omezuruike Okonko
Department of Virology
Faculty of Basic Medical Sciences
University of Ibadan
Ibadan, Nigeria.

Dr. Mike Agenbag
Municipal Health Services,
Joe Gqabi,
South Africa.

Dr. Abdel-Hady El-Gilany
Department of Public Health & Community Medicine, Faculty of Medicine
Mansoura University
Egypt.

Dr. Bachir Raho Ghalem
Biology Department,
Faculty of natural sciences and life,
Mascara university,
Algeria.

Table of Content

Effect of methylprednisolone on the morphology of acute lymphoblastic leukemia cell line in vitro model by Atomic Force Microscopy 202

Amairani Moreno-Caro, Edgar Sandoval-Petris, Josue Juarez, Miguel A. Valdez, Leonardo Ibor Ruiz-Ortega, Homero Rendón-García and María G. Burboa-Zazueta

Screening groundnut rhizobia for multiple plant growth promoting activities in Ethiopia 212

Asnake Beshah, Fassil Assefa, Driba Muleta and Gudina Legese

Density and diversity of arbuscular mycorrhizal fungi in Anacardium occidentale L. plantations in Senegal 221

Khémes Marie Odile THIOCONE, Abdoulaye SOUMARE, Mohamed Mahamoud CHARAHABIL, Landing NDIAYE, Fatou NDOYE, Saliou FALL, Valérie HOCHER4 and B. A. AMADOU

Vol. 17(9), pp. 202-211, September 2023
DOI: 10.5897/AJMR2023.9698
Article Number: 873D54A71167
ISSN: 1996-0808
Copyright©2023
Author(s) retain the copyright of this article
http://www.academicjournals.org/AJMR

ACADEMIC JOURNALS
expand your knowledge

African Journal of Microbiology Research

Full Length Research Paper

Effect of methylprednisolone on the morphology of acute lymphoblastic leukemia cell line *in vitro* model by Atomic Force Microscopy

Amairani Moreno-Caro[1], Edgar Sandoval-Petris[1], Josue Juarez[2], Miguel A. Valdez[2], Leonardo Ibor Ruiz-Ortega[4], Homero Rendón-García[3] and María G. Burboa-Zazueta[1]*

[1]Departamento de Investigaciones Científicas y Tecnológicas de la Universidad de Sonora, C.P. 83000, Hermosillo, Sonora México.
[2]Departamento de Física, Universidad de Sonora, C. P. 83000, Hermosillo, Sonora, México.
[3]Hospital Infantil del Estado del Sonora, Reforma 355, C. P. 83100 Hermosillo, Sonora, México.
[4]Department of Biological Sciences, Columbia University, New York, NY, 10027, USA.

Received 4 April, 2023; Accepted 24 August, 2023

Despite the recent knowledge of the molecular mechanisms of corticosteroid drugs in lymphoid leukemia, information about the nanostructured surface morphology of the process of cell death is limited. Therefore, the main objective of this work is to analyze the effect of methylprednisolone on the morphology of B lymphoblast CCRF-SB cell line by Atomic Force Microscopy (AFM). Morphological parameters such as height, cell diameter, and roughness were analyzed and used as indicator of cell surface damage. In accordance with AFM images, CCRF-SB cells show an ovoid shape, with a nucleus which occupies a great area of the cytoplasm delimited by the cellular membrane. When a CCRF-SB cells cell was exposed to the drug, the morphology of the cell changed. After 24 h, CCRF-SB cells remains in its ovoid shape; however, AFM images show irregularities that indicate disruption of the cellular membrane and the formation of cellular bodies in the cytoplasm and nucleus. Interestingly, AFM images showed dramatically changes in the morphology of the CCRF-SB cell after 48 h, where fragmentation of the cytoplasm and nucleus were recorded, as result of the cellular death process. These changes in the cellular morphology of CCRF-SB cell can be associated with the cell damage and death process caused by drugs such as methylprednisolone and can be used to control their effectiveness and to establish a correct diagnosis in cancer treatment.

Key words: Glucocorticoids, atomic force microscopy (AFM), cancer cells, CCRF-SB cell, roughness, nuclear cell fragmentation.

INTRODUCTION

Cancer was the cause of nearly 10 million deaths in 2020 in the world, which is nearly one in six of all deaths. The most common types of cancer in 2020 were: Breast (2.26 million), Lung (2.21 million), Colon (1.93 million), among

*Corrresponding author. E-mail: maria.burboa@unison.mx. Tel: +1 52 6621116567.

Author(s) agree that this article remain permanently open access under the terms of the Creative Commons Attribution License 4.0 International License

others (Chhikara and Parang, 2023).

Leukemia is the cancer of blood including white blood cells. There are different types of leukemia: acute lymphoblastic leukemia (ALL), acute myeloid leukemia (AML), and chronic lymphocytic leukemia (CLL); they all affect different age groups. Approximately 474,519 new cases of leukemia contributing 2.5% of total cancer appeared in 2020. Even when leukemia deaths were about 3.1% of all cancer deaths in 2020, leukemia is the most frequent cause of cancer death in children and persons younger than 39 years old (Chhikara and Parang, 2023). Of all leukemias, ALL has the major incidence (about 76%) with the highest rate in children less than 1 year old. Since time ago, leukemia treatments are based on chemotherapy with anthracyclines (Chhikara and Parang, 2010; Terwilliger and Abdul-Hay, 2017). Recently, there have been also important developments in drug delivery through nanotechnology formulations (Mayer et al., 2019) and new genetic technologies (Padmakumar et al., 2021).

Glucocorticoids are steroid hormones (Timmermans et al., 2019) used as anti-inflammatory and antineoplastic drugs, especially in hematologic malignancies.

The actions of glucocorticoids have been associated not only to their differentiation-inducing and apoptosis-inducing effects, but also to the modification of several steps of the hematopoietic and/or immune pathway and these have been reported (Yetgin and Özsoylu, 2007). Specifically, the activity of corticoids on lymphoid cells is described in three steps: initiation (the activation of corticosteroid on lymphocytes), decision step (degradation of pro-survival transcription factors, induction of apoptosis by caspase-3 activation, DNA fragmentation, among others), and the execution step (caspases and endonucleases are activated) (Distelhorst, 2002). Besides, it has been found that glucocorticoids are linked with other cellular mechanisms, such as the proteasomal inhibition, concentration changes of Ca, Na, and K ions (Greenstein et al., 2002; Smith and Cidlowski, 2010; Lambrou et al., 2012; Abdoul-Azize et al., 2017). Recent investigations of the effect of glucocorticoids on colitis and other types of cancer reported that their the rapeutical effectiveness remains questionable and suggested future research (Zhang et al., 2020; Mayayo-Peralta et al., 2021). In the case of ALL, Velentza et al. (2021) suggested the use of glucocorticoids to treat this disease, but not for long-term treatments, because of the children's bone health, among other collateral effects.

Methylprednisolone (MP) is one of the most utilized glucocorticoids drugs in the treatment of ALL (McNeer and Nachman, 2010). ALL is one oncological entity, which activates abnormal mechanisms of proliferation, maturation, and differentiation of lymphoid cells, leading to an increase of immature cells (blast) in the blood stream (Conter et al., 2004). ALL has a higher frequency in children population and is one of the most common leukemia reported (Larios-Farak et al., 2016). The most common treatment for ALL, as mentioned earllier, is the chemotherapy that is based on three steps: induction to the remission, consolidation, and maintenance (Kato and Manabe, 2018). Before the first step, steroids like methylprednisolone are supplied for 7 days, to classify the patients in groups, according to a good, regular, or bad response to the treatment (Tissing et al., 2003; Rendón-García et al., 2017).

Usually, the effects of MP have been investigated on the morphology of leukemia cells. These analyses have been restricted only to optical and electronic microscopy techniques (Hiçsönmez et al., 1996; Hiçsönmez et al., 1999; Özbek et al., 1999). However, it is important to investigate the effect of this drug on leukemia cells by analyzing the topographic characteristics (ultrastructure, diameter, height, roughness) with the intention of gaining a better understanding of the mechanisms of action of corticoids at a nanostructural level.

Atomic Force Microscopy (AFM) is commonly used to observe the surface structure of soft and solid materials (Zhao et al., 2019). It has a very sensitive and sharp probe attached at the edge of a microcantilever, very sensitive to small forces (Figure 1). When the tip is approaching the sample surface, atoms of the tip and the surface interact with a very weak force, but it is enough to perturb the oscillation of the cantilever; then, the position of the probe is detected by an optical sensor, converting this information in a topographical image. From this image, we obtain the relative height of a point to another one and the morphological characteristics from the surface of a given sample (Patel and Kranz, 2018). AFM offers a variety of methods allowing the study of the topography of cells with high resolution (Lastella et al., 2007; Wu et al., 2009; Francis et al., 2010). For instance, AFM was used to analyze the effect of a drug on the cell surface and evaluate the morphological changes in cancer cells with the aim of investigating the morphological changes in the death processes. Through the analysis of the topographic AFM images, it is possible to differentiate a healthy cell from a malignant one by comparing the topographical differences between these cells (Wang et al., 2009; Kim et al., 2012; Pillet et al., 2013; Deng et al., 2018). Specifically, this technique has been used to evaluate roughness and elasticity of cytoskeleton. Therefore, AFM is suitable for measurements to study cellular tissues in pathology (Cai et al., 2010; Jembrek et al., 2018). In the case of leukemia cells, AFM has been used to study the elastic properties of leukemia cancer cell membranes (Rosenbluth et al., 2006). They found that myeloid leukemias are involved in leukocytosis at a higher rate than lymphoid leukemias. A review by Li et al. (2021) shows the different uses of AFM as a tool for analysis of mechanical properties of cells, organelles, and biomolecules.

Thus, the main objective of this work is to measure the effects of MP on the morphology of cells CCRF-SB of

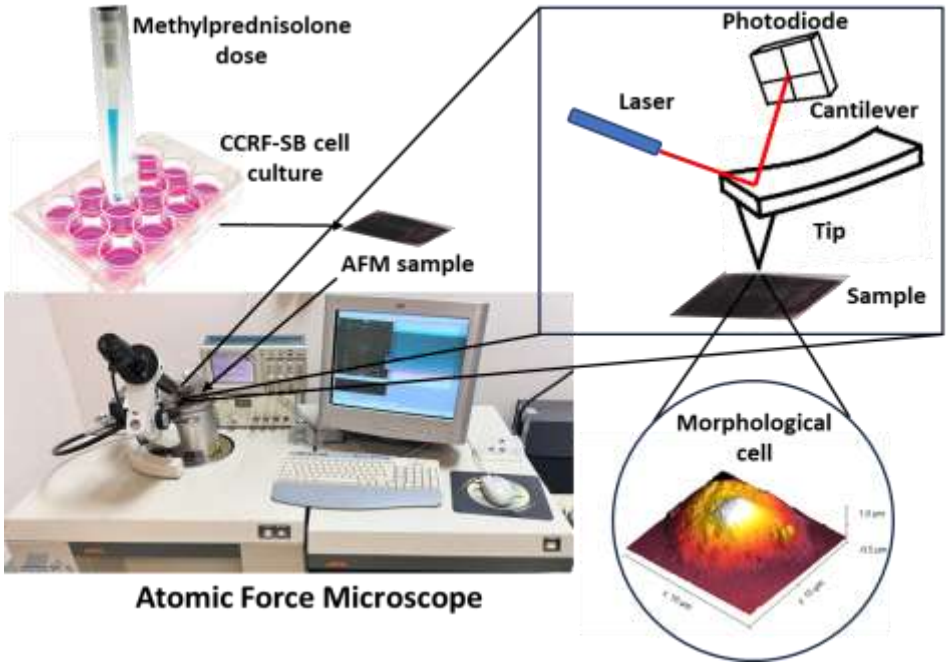

Figure 1. Set-up for an Atomic Force Microscopy. (AFM in the Complex Fluids Lab. University of Sonora)

LLA type B by AFM-based methods and use the parameters such as shape, diameter, height, and roughness to evaluate the cell death process. In general, AFM images show morphological changes such as nuclear and cell fragmentation observed in the cell membrane of CCRF-SB cells, whilst mean roughness (Ra) and mean square roughness (R_q) increased significantly after the drug exposure of 24 and 48 h. In this regard, CCRF-SB cells show an ovoid shape, with a nucleus which occupied a great area of the cytoplasm delimited by the cellular membrane. After 24 h of drug exposition, CCRF-SB cells retained its ovoid shape; however, AFM images show irregularities that indicate disruption of the cellular membrane and the formation of cellular bodies in the cytoplasm and nucleus. After 48 h, interestingly, the morphology of CCRF-SB cells changed and fragmentation of the cytoplasm and nucleus was observed, as a result of the cellular death process. On the other hand, the diameter and height recorded for CCRF-SB cells before the exposition of methylprednisolone were 19 and 0.88 µm, changing to 22 and 1.46 µm, respectively after 24 h of exposition; whilst after 48 h of drug exposition, the diameter and height recorded were 30 and 1.01 µm, respectively.

MATERIALS AND METHODS

Culture cell and methylprednysolone exposition

The B lymphoblast cell line CCRF-SB [CCRF SB] (ATCC ®CCL-120™) was purchased from American Type Culture Collection (ATCC) and used as model of acute lymphoblastic leukemia type B. This cell line has been widely used to investigate ALL, which is the most common type of cancer in childhood (Mendoza-Santiago et al., 2019; Zhao et al., 2020). The CCRF-SB cells were cultured under humidified atmosphere (80-100%) with 5% CO_2 and temperature 37°C. Cells were resuspended in RPMI 1640, supplemented with 10% of bovine fetal serum, amphotericin B 250 µg/ml, penicillin/streptomycin 10,000 IU/ml to 10,000 µg/ml ATCC, gentamycin of 50 mg/ml. Then, CCRF-SB cells were cultured in modified 12-well Petri dishes and exposed to a dose of 845 µM of MP for 24 and 48 h (Özbek et al., 1999).

Sample preparation for AFM analysis

Sterilized supports (mica 1 cm × 1 cm) were used and put in a Petri dish, where 40 µL of L-polylysine (Sigma Aldrich) was added and spread onto the whole surface. After 1 h, the sterilized supports were dried in an incubator. After drying, 50 µl of a CCRF-SB cell suspension (2.5 and 3.0 × 10^4 cells/ml) was added onto the mica surface, incubating for 20 min; after that, cells were fixed with 200 µl formaldehyde (4%) for 5 min.

The use of formaldehyde as a cell fixation agent has been controversial for several years. Szende and Tyihák_ (2010) found that formaldehyde promotes and inhibits the proliferation of cancer cells with different concentrations; Khoirunnisa et al. (2016) have investigated the molecular interaction of formaldehyde and proteins in human cancer cells. On the other hand, the use of formaldehyde as a crosslinking agent is well known (Hoffman et al., 2015) and as fixation agent of cells on solid surfaces, recommending 4% solutions in PBS up to 15 min (Thavarajah et al., 2012). Taking account, the effect of formaldehyde on cells mentioned earlier, we blocked the fixation process of formaldehyde after 5 min. The surface mica was washed three times with PBS (200 µl) and finally, with distilled water to avoid cell damage and the formation of

phosphate crystals during the drying process, prior to AFM observation (Canetta et al., 2014).

Atomic force microscopy

AFM images were recorded with a Jeol JSPM 4210 Japan AFM instrument (Figure 1) with a MikroMasch NSC15/NO AL cantilever with a nominal spring constant of 40 N/m and a resonance frequency around 325 Khz. Images were obtained in the non-contact mode, using a scan size of 70 µm × 70 µm acquired at a scan speed of 3.333 ms^{-1}. These scanning parameters were selected to get a panoramic AFM image with medium quality, in a time of 15 min, and find a CCRF-SB cell. Then after, a manual zoom was carried out on a CCRF-SB cell, and the AFM image was acquired at a scan size of 30 × 30 µm and scan speed of 10.000 ms^{-1}, to get a high-quality topographic image in approximately 45 min.

Surface roughness

The surface roughness (nm) of the samples was analyzed with two parameters: mean roughness (R_a) and mean square roughness (R_q) (Zhao, et al., 2019). R_a is calculated by:

$$R_a = \frac{1}{N_x N_y}\sum_{i=1}^{N_x}\sum_{j=1}^{N_y}\left|Z_{i,j} - Z_{av}\right| \quad , \quad \text{with}$$

$$Z_{av} = \frac{1}{N_x N_y}\sum_{i=1}^{N_x}\sum_{j=1}^{N_y} Z_{i,j} \, , \qquad (1)$$

On the other hand, R_q represents the relative change in the surface roughness of the sample, and it is given by:

$$R_q = \sqrt{\frac{1}{N_x N_y}\sum_{i=1}^{N_x}\sum_{j=1}^{N_y}(Z_{i,j} - Z_{av})^2} \qquad (2)$$

where N_x and N_y are the number of scanning points on the x-axis and y-axis of the AFM image, respectively, $Z_{i,j}$ is the height of the (i,j) point and Z_{av} is the average height of all measuring points from the surface AFM scanning image.

Then, R_a and R_q were determined by randomly sectioning the CCRF-SB cell from the high-quality topographic AFM image (30 × 30 µm) in smaller areas (2 × 2 µm). The cellular sections with artifacts were discarded for roughness analysis.

Data analysis

Software Gwyddion (Nečas and Klapetek, 2012) was used to visualize the morphological parameters of CCRF-SB cells, while quantitative parameters, such as height, diameter, roughness Ra and Rq were determined with the WsxM 5.0 software program (Horcas et al., 2007). The height, diameter, and roughness (Ra and Rq) of CCRF-SB cells were analyzed by one-way nonparametric ANOVA (Kruskal-Wallis) by Minitab Statistical software. This statistical analysis is recommended for small samples, and it is used to determine if there are significant differences between quantitative variables of at least three independent groups. In this case, four AFM images coming from four independent CCRF-SB cells non-exposed and exposed to a dose of MP (845 µM) for 24 and 48 h were analyzed. After nonparametric ANOVA analysis, a post-Hoc test (Tukey) was carried out to determine the statistical significance among data, considering the p values minor to α, the typical significance level (α <0.05).

RESULTS AND DISCUSSION

Ultra structure of CCRF-SB cells

Drugs, viruses, bacteria, etc., can kill a given cell. During the cell death process, the integrity of the cell is damaged modifying its morphological parameters; therefore, in order to understand the death cell process produced by a specific drug, *in vitro* experiments can be conducted to study the cell morphology (Huang et al., 2014).

In this regard, we have investigated the effect of methylprednisolone on the morphology and ultrastructure of CCRF-SB cells, as a B lymphoblast cell model. Lymphoblasts are non-adherent cells, almost always ovoid round shape; these cells are bigger than lymphocytes with a larger cell proportion occupied by the nucleus. It is common to find cells with two nucleoli and cytoplasmic vacuoles.

Figure 2 shows the morphological characteristic of a CCRF-SB cell. It can be observed as a CCRF-SB cell (Figure 2, Image 1) with ovoid round shape, limited by the cell membrane, which result like the shape for health lymphocytes observed by optical microscopy (Laane et al., 2009). Heights of cells are between 1 and 1.5 µ and diameters between 6 and 8 µ. At the nanostructure level (Figure 2, Images 1.1, 1.2, 2.1 and 2.2), we observe components homogeneously distributed along the plasmatic membrane, probably due to the presence of carbohydrates and proteins, which contribute to the structural support of cell membrane (Hu et al., 2009; Huang et al., 2014). Additionally, Figure 2 shows images of CCRF-SB cell in three dimensions (Images 1.3 and 2.3), in which a big nucleus/cytoplasm ratio and protrusions at the edge of the cell membrane can be observed.

Figures 3 and 4 show the AFM images recorded for CCRF-SB cell treated with 845 µM dose of MP after 24 and 48 h, respectively. Changes can be observed in the cell morphology as well as in the ultrastructure of lymphoblasts. Images 3 and 4 in Figure 3 correspond to cells exposed to MP after 24 h. As observed, the morphological changes were small at this time of treatment. On one hand, Images 3.1, 3.2, 4.1 and 4.3 show irregularities on the nucleus of CCRF-SB cell, such gaps (pink arrow in Image 3.1) or pores (Image 4.2). Additionally, in Image 4.3, swelling of cells and invaginations at the edge of the membrane can be observed (yellow arrow, Image 4.3). We note a large increase in cell height, the collapse of the membrane (green arrow, Image 3.3), and the presence of cellular bodies, because of the cellular death process (black arrow in Image 4.3).

The most significant changes in the morphology of

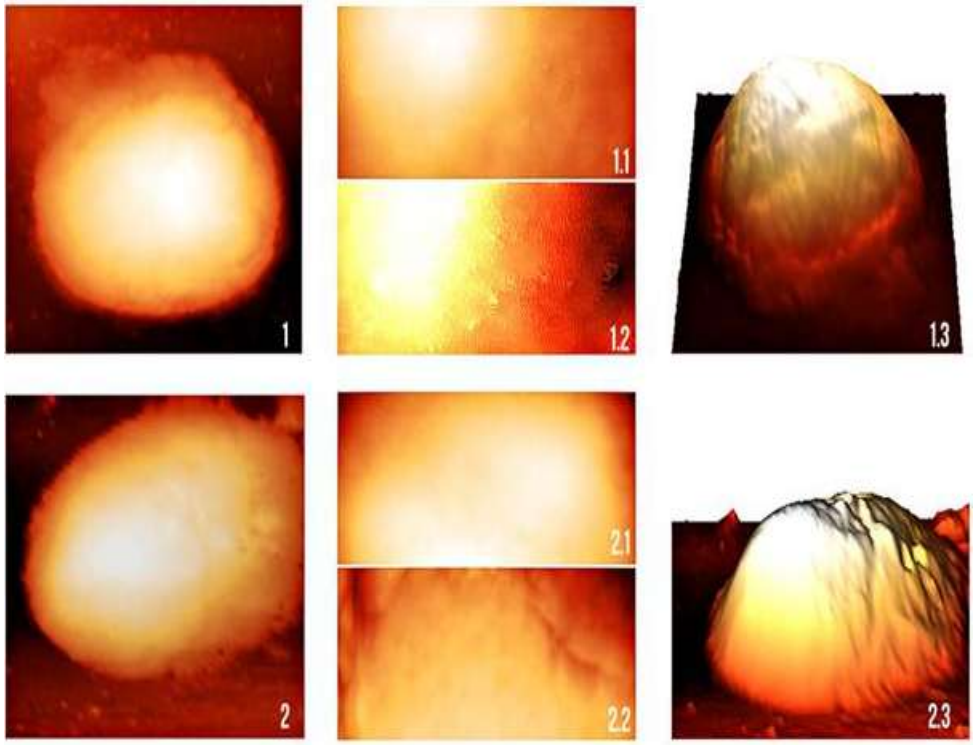

Figure 2. Representative images of the CCRF-SB cell line from a control cell group. Images 1 and 2 correspond to the topographies of the control cells, Images 1.1, 1.2, 2.1, and 2.2 correspond to scanning of 3 × 5 µm and Images 1.3 and 2.3 represents the three-dimensional (3D) cellular structure. Cell 1: Representative control cell, correspond to CCRF-SB without any treatment. 1.1: the ultrastructure of the nucleus, 1.2: ultrastructure of cellular cytoplasm. 1.3: 3D cell morphology. Cell 2: Representative control cell, 2.1: approach in the ultrastructure of the nucleus, 2.2: ultrastructure of cellular cytoplasm and 2.3: 3D morphology of CCRF-SB 2. Images were recorded with a Jeol JSPM 4210 Japan AFM instrument with a nominal spring constant of 40 N/m and a resonance frequency around 325 Khz.

CCRF-SB cell were observed after 48 h in the presence of MP. Some structures can be observed that may be vestiges of cell organelles, even though complementary techniques must be done (White arrow, Figure 4, Image 5.3). The nucleus fragmentation is more evident at the ultrastructure level (Images 6.1 and 6.2); the gap in Image 6.3 showed shrinking of the cell and deep depressions in the membrane cell (red arrow, Image 6.3), such as occurs in the cell necrosis process. Similar effects were also observed in myeloid leukemia cells k-562 exposed to dexamethasone (Wang et al., 2016). Changes on the cellular structure, as well as the formation of cytoplasmatic vacuoles, membane pores, cell shrinkage, protrusions at the edge of the membrane, smooth membrane and irregular nanostructure after the interaction with the drug were also observed. The presence of these damages can result from the apoptotic, necrotic and necroptotic processes (Hu et al., 2009).

On the other hand, we analyzed the morphology of CCRF-SB cell, to understand cellular death processes. Typically, in the cellular death process by apoptosis, the cell shows usual damages like loss of volume, cell shrinkage, apoptotic bodies, and DNA fragmentation. While, in the cell death by necrosis, cytolytic inflammation was observed, loss of membrane integrity, and cellular swelling cause an increase in the cell size. The necroptosis process is a combination of apoptosis and necrosis, both of which demand on a process called autophagy which uses lysosomes to wrap cytoplasm and organelles to make possible cell renewal processes and homeostasis (Walsh and Edinger, 2010). The necroptosis shows different effects on cells; blister-like structures on the cell membranes, cell shrinkage, chromatin condensation and apoptotic bodies formation without membrane rupture. Similarly, drugs of the glucocorticoid's family can activate the apoptosis intrinsic way, as well as the activation of the recruitment mechanism of the ionic channels of Ca^{2+} y Na^{+}, promoting the development of pores on the membrane (Smith and Cidlowski, 2010); therefore, supporting the theory of pores on the membrane, developed by Schwartzman and Cidlowski (1994). They describe the action mechanism of glucocorticoids, which destabilize the plasmatic membrane by a lysis process through pores of

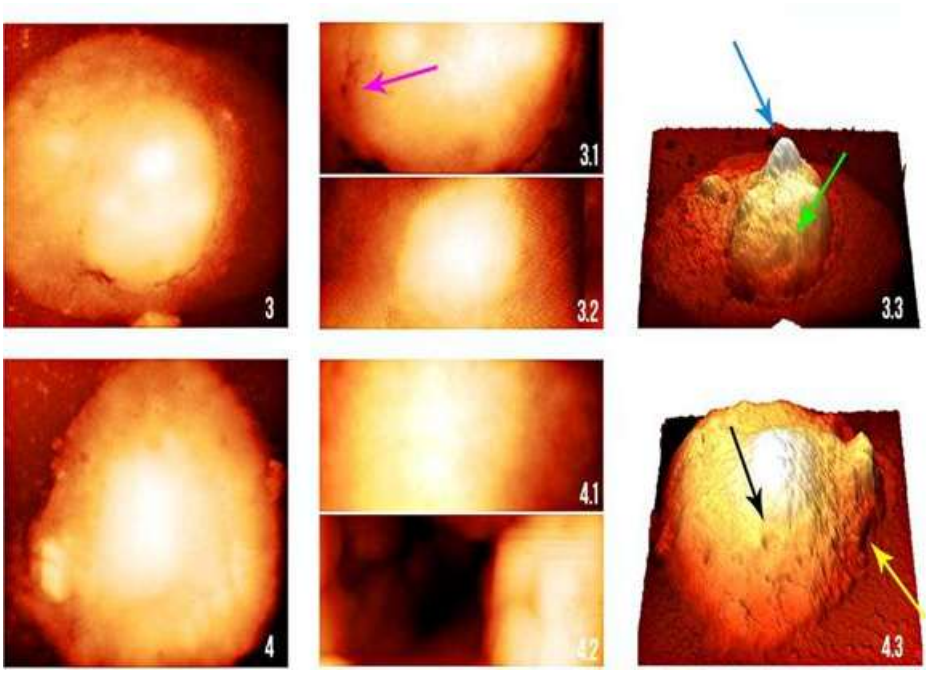

Figure 3. Representative images of the CCRF-SB cell after 24-h exposure with Methylprednisolone. The first column corresponds to the cell topographies, second corresponds to approach of 3 × 5 µm and the third represents the 3D cellular structure. Image 3: Group cell 24 h. Image 3.1: approach in the ultrastructure of the nucleus, pink arrow indicates irregularities in peripheral nuclear membrane, Image 3.2: ultrastructure of cellular cytoplasm. Image 3.3: 3D cell morphology, blue arrow, early nuclear fragmentation, green arrow, nuclear clefts. Image 4: Representative cell of the group 24 h, Image 4.1: approach in the ultrastructure of the nucleus, Image 4.2: cytoplasmic ultrastructure, with special focus on 800 × 800 nm cytoplasmic pore and Image 4.3: 3D morphology of Lymphoblast 4, black arrow, pore location figure 4.2, yellow arrow, early invagination in cytoplasm.

membrane caused by an increase of Ca^{2+} in the cell processes, provoking a concentration difference through the membrane (Pan et al., 2016).

Morphological parameters

Height and diameter

These parameters were analyzed with a non-parametric ANOVA program. The height profile was defined as the difference between the tallest point of cells and the bottom. Results showed non-significant differences between control CCRF-SB cell and cells treated with MP after 24 and 48 h (Table 1). The control cell showed an average height of 0.88 µ and an average diameter of 1.46 µm and 1.01 µm after 24 and 48 h MP of treatment with MP treatment, respectively. Similar results have been reported by Huang et al. (2014), who observed changes in the height of lymphocytes treated with aminophylline for 48 h. These results suggest that the integrity of the cell membrane has been affected due to the MP exposition, affecting the biological characteristic, such as height, diameter, and roughness (Ra and Rq), and eventually, the physiological function of cells (Huang et al., 2014).

Roughness

Roughness is a cytological parameter because it is related with cell processes like cell mechanics, which is also related with adhesion and motility (Antonio et al., 2012); therefore, it is a sensible parameter for the measurement of the state of cells and is intimately bounded with the integrity of the cytoskeleton and the processes that produce structure changes. Then, the change of diameter, height and roughness parameters can be used as a damage sensor in the cell membrane when cells are under cellular death process (apoptosis, necrosis, or necroptosis processes) (Liu et al., 2018).

Roughness values were obtained on random way in section of 2 × 2 µm, neglecting every cell artifact. Figure 5 shows that both Ra and Rq displayed significant differences between non-treated CCRF-SB cells and treated CCRF-SB cells with MP after 24 and 48 h. The

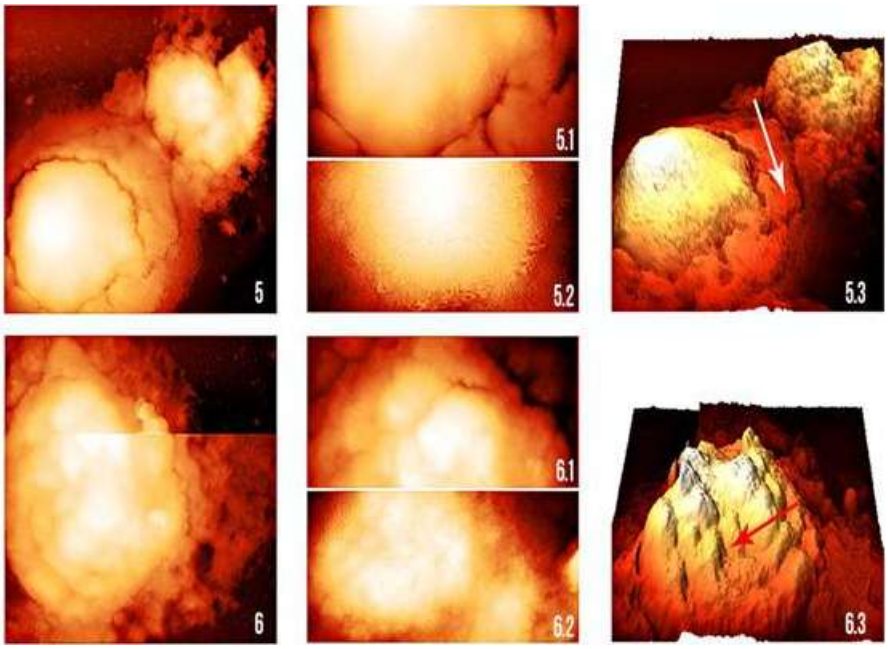

Figure 4. Representative images of CCRF-SB cell with a 48-h exposure time to Methylprednisolone. The first column corresponds to the cellular topographies, the second approach of 3 × 5 µm, and the third representation of the 3D cellular structure. Cell Image 5: Representative cell of the group 48 h. Image 5.1: approach in the ultrastructure of the nucleus, with long fragmentation lines in the peripheries of the nucleus, Image 5.2: ultrastructure of cellular cytoplasm. Image 5.3: 3D cell morphology, white arrow advanced cytoplasmic fragmentation, with cell rupture. Image 6: representative cell of the group 48 h, Image 6.1: approach in the ultrastructure of the nucleus with nuclear fragmentation. Image 6.2: ultrastructure of cytoplasm, and Image 6.3: 3D morphology of Lymphoblast.

Table 1. Cellular size after CCRF-SB cell was exposed to methylprednisolone for 24 and 48 h.

Time of exposition (h)	Diameter (µm) + SD	Height (µm) + SD
0	19 ± 3	0.88 ± 0.07
24	22 ± 6	1.46 ± 0.70
48	30 ± 6	1.01 ± 0.22

Data represent mean of diameter and height. Each group represents the measurements of 4 cells. SD: Standard deviation.

results obtained in this investigation for Ra were 79 ± 15 nm for the control group, 133.4 ± 29.4 nm for cells CCRF-SB with MP exposed 24 h and for cells exposed 48 h was 122.3 ± 16.7 nm. The values of Rq were 93 ± 17, 159.3 ± 34.5, and 141.4 ± 15.4 nm, respectively for the control and the two treatments. These changes in the Ra and Rq values can result from different cellular processes in which the integrity of the cell membrane is compromised. In this regard, Dong et al. (2013) reported changes in the cellular roughness (Ra and Rq) of leukemia lymphoid cells type B exposed to *Staphylococcus aureus*. They observed that the Ra value increased to 3.18 ± 0.35 and 3.07 ± 0.18 nm after the cells were exposed to the Gram (+) bacteria for 24 and 72 h, respectively. While the Rq roughness registered was around 3.93 ± 0.08 and 3.47 ± 0.31 nm, respectively. Dong et al. (2013) explained that the observed changes in Ra and Rq have resulted from the redistribution of the components of the cell membrane that takes place at the surface of the cell (Dong et al., 2013).

Besides the contribution of AFM to the evaluation of changes caused on the morphology and mechanical properties by anticancer drugs on cancer cells, and help to obtain a diagnosis of cancer, there are many other uses of AFM in investigations at molecular level. However, AFM cannot investigate the chemical composition of cells

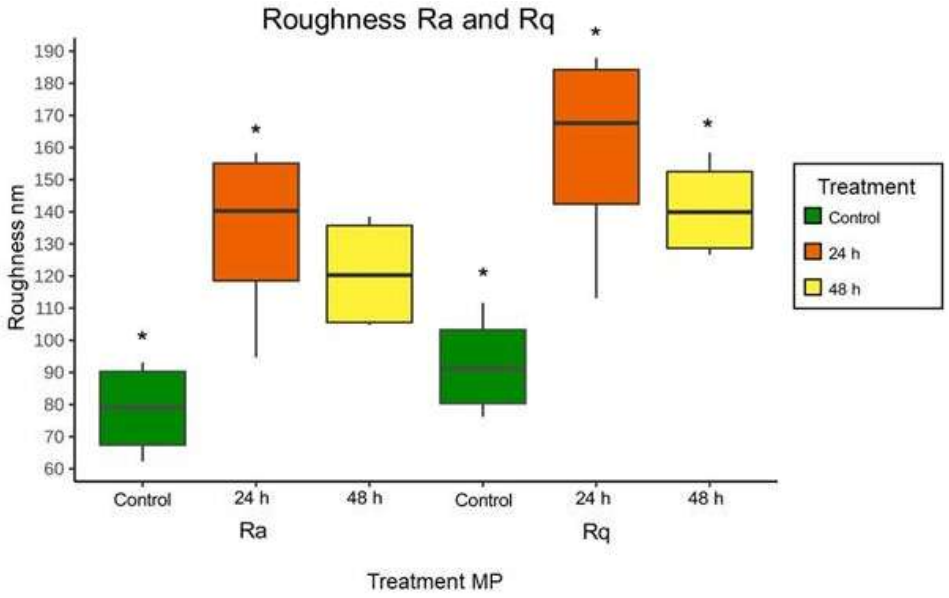

Figure 5. Box plot for cell roughness Ra and Rq subjected to three treatments, control group, treatment with MP at 24 and 48 h. Results represent mean +/- SD of Ra and Rq. Each group represents the measurements in cm/nm/pixel of 4 cells. One-way nonparametric ANOVA (Kluskal-Wallis) followed by Tukey test were used to analyze the Ra and Rq parameters and to compare control cells and cells treated with MP for 24 and 48 h ($p<0.05$).

or molecules and sometimes it is slow to get information on damaged cells, but combined with other techniques like Raman spectroscopy, scanning microscopy confocal laser scanning microscopy, scanning electron microscopy, among others, AFM offers an excellent tool to obtain more precise diagnosis of cancer cells (Deng et al., 2018).

Conclusions

The effects of methylprednisolone (MP) on the morphological properties of leukemia B cell model (CCRF-SB cell line, CCRF-SB) were evaluated by AFM. Before the AFM analysis, a protocol to fix the CCRF-SB CCRF-SB cell onto the mica surface was standardized. It is important to remark that this approach allows to determine the effects of the exposition of MP (845 µM) on the morphology of CCRF-SB cell CCRF-SB by AFM, taking into count parameters such diameter, height, morphology, and roughness. Since these parameters give information about the integrity of the cell membrane, then they have potentials as biomarkers useful to analyze the cellular damages after the exposition of a given drug. In this regard, AFM images allowed to observe the loss of ovoid shape of CCRF-SB cell after cells were exposed to MP for 24 and 48 h. Additionally, despite CCRF-SB retaining its ovoid shape, the exposition to MP for 24 h, topographical irregularities were observed, suggesting that the integrity of the cell membrane has been affected by the exposition to the drug, causing the disruption of the cellular membrane and the formation of cellular bodies in the cytoplasm and nucleus. These effects were more evident after 48 h of exposition to MP, observing fragmentation of the cytoplasm and nucleus of CCRF-SB cells, indicating that cells are dying. These results suggest that the AFM can be considered a powerful tool to study the morphology and topography of cells after the exposition of a given drug. However, AFM tool is limited to be applied in research areas, and it is difficult to be used for clinical purposes due to the time required to prepare the cell sample and to acquire images with high resolution (at least 45 min per image).

CONFLICT OF INTERESTS

The authors have not declared any conflict of interests.

ACKNOWLEDGEMENTS

The authors are grateful to Consejo Nacional de Humanidades, Ciencia y Tecnología (CONAHCYT) for the economic and CONAHCyT (Projects # 2264, 236185, 241133) for the financial support.

REFERENCES

Abdoul-Azize S, Dubus I, Vannier J (2017). Improvement of dexamethasone sensitivity by chelation of intracellular Ca^{2+} in pediatric acute lymphoblastic leukemia cells through the prosurvival kinase ERK1/2 deactivation. Oncotarget 8(16):27339-27352.

Antonio PD, Lasalvia M, Perna G, Capozzi V (2012). Scale-independent roughness value of cell membranes studied by means of AFM technique. Biochimica et Biophysica Acta 1818(12):3141-3148.
Cai X, Xin X, Cai J, Chen Q, Wu S, Huang F (2010). Connection between biomechanics and cytoskeleton structure of lymphocyte and Jurkat cells: An AFM study. Micron 41(3):257-262.
Canetta E, Riches A, Borger E, Herrington S, Dholakia K, Adya AK (2014). Discrimination of bladder cancer cells from normal urothelial cells with high specificity and sensitivity: combined application of atomic force microscopy and modulated Raman spectroscopy. Acta biomaterialia 10(5):2043-2055.
Chhikara BS, Parang K (2010). Development of cytarabine prodrugs and delivery systems for leukemia treatment. Expert Opinion on Drug Delivery 7(12):1399-1414.
Chhikara BS, Parang K (2023). Global Cancer Statistics 2022: the trends projection análisis. Chemical Biology Letters 10(1):451.
Conter V, Rizzari C, Sala A, Chiesa R, Citterio M, Biondi A (2004). Acute Lymphoblastic Leukemia. Orphanet Encyclopedia 10(4):11-25.
Deng X, Xiong F, Li X, Xiang B, Li Z, Wu X, Xiong W (2018). Application of atomic force microscopy in cancer research. Journal of Nanobiotechnology 16(1):102.
Distelhorst C (2002). Recent insights into the mechanism of glucocorticosteroid-induced apoptosis. Cell Death & Differentiation 9(1): 6-19.
Dong S, Wang Q, Sun S, Liang Y, Jiang J, Liu L (2013). Atomic force microscopy of chronic lymphatic leukaemia cells activation induced by Staphylococcus aureus. Cell Biology International 37(4):380-386.
Francis LW, Lewis PD, Wright CJ, Conlan RS (2010). Atomic force microscopy comes of age. Biology of the Cell 102(2):133-143.
Greenstein S, Ghias K, Krett N, Rosen S (2002). Mechanisms of Glucocorticoid-mediated Apoptosis in Hematological Malignancies. Clinical Cancer Research 8:1681-1694.
Hiçsönmez G, Erdemli E, Tekelioglu M, Tuncer A, özbek N, Cetin M, Cotter T (1996). Morphologic Evidence of Apoptosis in Childhood Acute Myeloblastic Leukemia Treated with High-Dose Methylprednisolone. Leukemia & Lymphoma 22(1-2): 91-96.
Hiçsönmez G, Tuncer M, Toksoy H, Yenicesu I, Çetin M (1999). Differentiation of Leukemic Cells Induced by Short-Course High-Dose Methylprednisolone in Children with Different Subtypes of Acute Myeloblastic Leukemia. Leukemia & Lymphoma 33(5-6):573-580.
Hoffman EA, Brian L. Frey BL, Smith LM, Auble DT (2015). Formaldehyde Crosslinking: A Tool for the Study of Chromatin Complexes. The Journal of Biological Chemistry 290(44):26404-26411.
Horcas I, Fernández R, Gómez-Rodríguez J, Colchero J, Gómez-Herrero J, Baro A (2007). WSXM: A software for scanning probe microscopy and a tool for nanotechnology. Review of Scientific Instruments 78(1):13705.
Hu M, Wang J, Zhao H, Dong S, Cai J (2009). Nanostructure and nanomechanics analysis of lymphocyte using AFM: from resting, activated to apoptosis. Journal of biomechanics 42(10):1513-1519.
Huang X, He J, Liu M, Zhou C (2014). The influence of aminophylline on the nanostructure and nanomechanics of T lymphocytes: an AFM study. Nanoscale Research Letters 21 9(1):518.
Jembrek M J, Vlainić J, Čadež V, Šegota S (2018). Atomic force microscopy reveals new biophysical markers for monitoring subcellular changes in oxidative injury: Neuroprotective effects of quercetin at the nanoscale. PLOS ONE 13(10):1-22.
Khoirunnisa W, Puspitarini S, Rohmawati SA, Eltavia F, Rahayu RP, Utomo DH, Permatasari GW (2016). Molecular mechanism of formaldehyde and protein interaction in human cancer cell. Trends in Bioinformatics 9:30-34.
Kim K, Cho C, Park E, Jung M, Yoon K (2012). AFM-Detected Apoptotic Changes in Morphology and Biophysical Property Caused by Paclitaxel in Ishikawa and HeLa Cells. Plos One 7(1):1-9.
Kato M, Manabe A (2018). Treatment and biology of pediatric acute lymphoblastic leukemia. Pediatrics International 60(1):4-12.
Laane E, Tamm KP, Buentke E, Ito K, Kharaziha P, Oscarsson J, Corcoran M, Bjo¨ rklund A-C, Hultenby K, Lundin J, Heyman M, So¨ derha¨ll S, Mazur J, Porwit A, Pandolfi PP, Zhivotovsky B, Panaretakis T and Grande´r D (2009). Cell death induced by dexamethasone in lymphoid leukemia is mediated through initiation of autophagy. Cell Death and Differentiation 16:1018-1029.
Lambrou G, Papadimitriou L, Chrousos G, Vlahopoulos S (2012). Glucocorticoid and proteasome inhibitor impact on the leukemic lymphoblast: Multiple, diverse signals converging on a few key downstream regulators. Molecular and Cellular Endocrinology 351(2):142-151.
Larios-Farak TC, Rendón-García H, Ornelas-Ceballos JR, Covarrubias-Espinoza G, Ríos-García CG, Morales-Peralta A (2016). Supervivencia de niños con Leucemia Linfoblástica Aguda de riesgo intermedio. Boletín clínico del Hospital Infantil del Estado de Sonora 33(1):19-25.
Lastella M, Lasalvia M, Perna G, Biagi PF, Capozzi V (2007). Atomic force microscopy study on human keratinocytes treated with HgCl2. Journal of Physics: Conference Series 61(1):920.
Li M, Xi N, Wang Y, Liu L (2021). Atomic force microscopy for revealing micro/nanoscale mechanics in tumor metastasis: from single cells to microenvironmental cues. Acta Pharmacologica Sinica 42:323-339.
Liu J, Qu Y, Wang G, Wang X, Zhang W, Li J, Jiang J (2018). Study of morphological and mechanical features of multinuclear and mononuclear SW480 cells by atomic force microscopy. Microscopy research and technique 81(1):3-12.
Mayayo-Peralta I, Zwart W, Prekovic S (2021). Duality of glucocorticoid action in cancer: tumor-suppressor or oncogene?. Endocrine-Related Cancer 28:157-171.
Mayer LD, Tardi P, Louie AC (2019). CPX-351: A nanoscale liposomal co-formulation of daunorubicin and cytarabine with unique biodistribution and tumor cell uptake properties. International Journal of Nanomedicine 14: 3819-3830.
McNeer J, Nachman J (2010). The optimal use of steroids in pediatric acute lymphoblastic leukemia: no easy answers. British Journal of Hematology 149(5):638-652.
Mendoza-Santiago A, Becerra E, Garay E, Bah M, Berumen-Segura L, Escobar-Cabrera J, Hernández-Pérez A, García-Alcocer G (2019). Glutamic Acid Increased Methotrexate Polyglutamation and Cytotoxicity in a CCRF-SB Acute Lymphoblastic Leukemia Cell Line. Medicina 55:758.
Nečas D, Klapetek P (2012). Gwyddion: an open-source software for SPM data analysis. Open Physics 10(1):181-188.
Özbek N, Erdemli E, Hiçsönmez G, Okur H, Tekelioğlu M (1999). Effects of Methylprednisolone on Human Myeloid Leukemic Cells In Vitro. American Journal of Hematology 60:255-259.
Padmakumar D, Chandraprabha VR, Gopinath P, Devi ARTV, Anitha GR J, Sreelata MM, Padmakumar A, Sreedharan H (2021). A concise review on the molecular genetics of acute myeloid leukemia. Leukemia Research 111:106727.
Pan Y, Liu XY, Liu JQ, Liu Q, Yang Y, Yang JL, Wang YZ (2016). Necroptosis: a new link between cell death and inflammation. Neuroimmunology Neuroinflammation 3:156-160.
Patel AN, Kranz C (2018). Multi-functional Atomic Force Microscopy Imaging. Annual Review of Analytical Chemistry 11:329-350.
Pillet F, Chopinet L, Formosa C, Dague É (2013). Atomic Force Microscopy and pharmacology: From microbiology to cancerology. Biochimica et Biophysica Acta 1840:1028-1050.
Rendón-García H, Tamayo-Pedraza G, Covarrubias-Espinoza G (2017). Ventana de esteroide en niños con Leucemia Linfoblástica Aguda evaluada por factores pronósticos. Boletín Clínico del Hospital Infantil del Estado de Sonora 34(2):82-89.
Szende B, Tyihák E (2010). Effect of formaldehyde on cell proliferation and death. Cell Biology International 34(12):1273-1282.
Smith L, Cidlowski J (2010). Glucocorticoid-Induced Apoptosis of Healthy and Malignant Lymphocytes. Neuroendocrinology – Pathological Situations and Diseases 148:1-30.
Schwartzman RA, Cidlowski JA (1994). Glucocorticoid-induced apoptosis of lymphoid cells. International Archives of Allergy and Immunology 105(4):347-354.
Terwilliger T, Abdul-Hay M (2017). Acute lymphoblastic leukemia: a comprehensive review and 2017 update. Blood Cancer Journal 7:e577.
Thavarajah R, Mudimbaimannar VK, Elizabeth J, Rao UK, Ranganathan K (2012). Chemical and physical basics of routine formaldehyde fixation. Oral Maxillofacial Pathology 16(3):400-405.
Timmermans S, Souffriau J, Libert C (2019). A General Introduction to

Glucocorticoid Biology. Fronteirs in Immunolgy Section Inflammation 10:1545.
Tissing W, Meijerink J, den Boer M, Pieters R (2003). Molecular determinants of glucocorticoid sensitivity and resistance in acute lymphoblastic leukemia. Leukemia 17(1):17-25.
Velentza L, Zaman F, S¨avendahl L (2021). Bone health in glucocorticoid-treated childhood acute lymphoblastic leukemia. Critical Reviews in Oncology/Hematology 168:103492.
Walsh CM, Edinger AL (2010). The complex interplay between autophagy, apoptosis, and necrotic signals promotes T-cell homeostasis Immunology Review 236: 95-109.
Wang J, Wan Z, Liu W, Li L, Ren L, Wang X, Zhang Z (2009). Atomic force microscope study of tumor cell membranes following treatment with anti-cancer drugs. Biosensors and Bioelectronics 25(4):721-727.
Wang Y, Xu C, Jiang N, Zheng L, Zeng J, Qiu C, Xie S (2016). Quantitative analysis of the cell-surface roughness and viscoelasticity for breast cancer cells discrimination using atomic force microscopy. Scanning 38:558-563**.**
Wu Y, Lu H, Cai J, He X, Hu, Y, Zhao H, Wang X (2009). Membrane Surface Nanostructures and Adhesion Property of T Lymphocytes Exploited by AFM. Nanoscale Research Letters 4(8):942-947.
Yetgin S, Özsoylu S (2007). Comparison of Megadose Methylprednisolone Versus Conventional Dose Prednisolone in Hematologic Disorders. Journal of Pediatric Hematology/ Oncology 29(4):253-259.
Zhang Z, Dong L, Jia A, Chen X, Yang Q, Wang Y, Wang Y, Liu R, Cao Y, He Y, Bi Y, Liu G (2020). Glucocorticoids Promote the Onset of Acute Experimental Colitis and Cancer by Upregulating Mtor Signaling in Intestinal Epithelial Cells. Cancers 12:945.
Zhao S, Li Y, Wang Y, Ma Z, Huang X (2019). Quantitative study on coal and shale pore structure and surface roughness based on atomic force microscopy and image processing. Fuel 244:78-90.
Zhao W, Li Y, Yao C, Zhang G, Zhao KY, Chen W, Ru P, Pan X, Tu H, Jones D (2020). Detection of Pathogenic Isoforms of IKZF1 in Leukemic Cell Lines and Acute Lymphoblastic Leukemia Samples: Identification of a Novel truncated IKZF1 Transcript in SUP-B15, 2020. Cancers 12(11):3161.

Vol. 17(9), pp. 212-220, September 2023
DOI: 10.5897/AJMR2023.9702
Article Number: 4299D4A71220
ISSN: 1996-0808
Copyright©2023
Author(s) retain the copyright of this article
http://www.academicjournals.org/AJMR

African Journal of Microbiology Research

Full Length Research Paper

Screening groundnut rhizobia for multiple plant growth promoting activities in Ethiopia

Asnake Beshah*, Fassil Assefa, Driba Muleta and Gudina Legese

Department of Cellular, Microbial and Molecular Biology, Addis Ababa University, Addis Ababa, Ethiopia.

Received May 20, 2023; Accepted 10 August, 2023

Rhizobia could exhibit plant growth-promoting mechanisms besides nitrogen fixation. In search of efficient rhizobia with multiple PGP traits, 72 groundnut nodulating rhizobia isolates were screened in vitro for their plant growth promoting traits like phosphate solubilization, production of indole acetic acid, ammonia, hydrogen cyanide, production of different hydrolytic enzymes and antifungal activity. About 72% of the isolates produced IAA, varying from 7.4 to 78.8 µg.ml^{-1} and 23.6% of the isolates were able to solubilize tri-calcium phosphate. Even if all isolates could produce ammonia, two isolates were strongly produced. Only two isolates were able to produce hydrogen cyanide. The enzymatic production study revealed that 50 and 48% of the tested isolates showed protease, and cellulase activities respectively. Only 13.8% of the isolates were found to be inhibitory against the test pathogen, *Fusarium oxysporum*, but the maximum inhibition potential was exhibited by GNR-07. The present study also demonstrated that 100% of the isolates exhibited multiple PGP (plant growth promotion) properties, with isolates GNR-37 and GNR-28 being superior, acquiring the highest number of PGP properties (87.5% each). These isolates can be potential candidates as a PGPR inoculant after evaluation of their performance under greenhouse and field conditions.

Key words: Rhizobia isolates, plant growth-promoting traits, enzymes and some chemical compound production, antifungal activity.

INTRODUCTION

Plant growth promoting rhizobacteria (PGPR) are a heterogeneous group of bacteria that can be found in the rhizosphere, at root surfaces and in association with roots, which can improve the extent or quality of plant growth directly and or indirectly (Meena et al., 2012; Moustaine et al., 2017). PGPR include different genera of bacteria such as *Acetobacter, Acinetobacter, Alcaligenes, Arthrobacter, Azoarcus, Azospirillum, Azotobacter, Bacillus, Beijerinckia, Burkholderia, Derxia, Enterobacter, Gluconacetobacter, Herbaspirillum, Klebsiella, Ochrobactrum, Pantoae, Pseudomonas, Rhodococcus, Serratia, Stenotrophomonas* and *Zoogloea* (Jha and Saraf, 2015).

PGPR can promote plant growth by both direct and indirect mechanisms. Direct mechanisms are defined as employing those bacterial traits that result in the direct promotion of plant growth. It includes the production of ACC deaminase, auxin, gibberellin, cytokinin, phosphorous solubilization, nitrogen fixation and impounding of iron by siderophore producing bacteria.

*Corresponding author: E-mail: asnake.beshah@yahoo.com.

Author(s) agree that this article remain permanently open access under the terms of the Creative Commons Attribution License 4.0 International License

The bacteria have characteristics that involve inhibiting the functioning of one or more plant pathogenic microorganisms, including fungi and bacteria. Indirect mechanisms include the production of cell wall degrading enzymes, antibiotics, competition, induced systemic resistance, hydrogen cyanide, quorum quenching, and siderophores (Olanrewaju et al., 2017). PGPR antagonize phyto-pathogens through various mechanisms; like competition for nutrients and space, production of antibiotics, production of lytic enzymes and hydrogen cyanide (Hamid et al., 2021; Jayaprakashvel et al., 2019; Kaur et al., 2021). Some bacteria produce enzymes such as chitinases, cellulases, proteases, and lipases that lyse and destroy cell walls of bacteria and fungi that are pathogenic for the plant. PGPR are capable to synthesize one or more of these enzymes have been found to have biocontrol activity against a range of pathogenic fungi (Sathya et al., 2017).

Rhizobia that form root nodules and fix atmospheric nitrogen with leguminous plants are one of the PGPR that possess many distinct plant growth-promoting traits that enhance plant growth of both leguminous and non-leguminous crops (Jaiswal et al., 2021; Knežević et al., 2022). Rhizobia can enhance plant growth directly through production of different metabolites having a property of plant growth promotor and biocontrol by production of different lytic enzymes (Gopalakrishnan et al., 2015).

It is reported that rhizobia nodulating groundnut host possess plant growth promoting (PGP) properties such as solubilization of inorganic phosphate (Afzal and Asad, 2019) phytohormone production such as Indole Acetic Acid (IAA) (Kumar et al., 2014; Panigrahi et al., 2020) and siderophore production (Vargas et al., 2017).

In general, root nodule rhizobia possessing multiple PGP traits confer additional advantage to serve as inoculants for both legume and non-legume crops grown rotationally or simultaneously. However, the number of studies on groundnut rhizobia is limited compared to other pulses, despite the growing commercial interest in crop production in Ethiopia. Hence, to improve the yield of groundnut, there is a need to collect, isolates, and screen more groundnut rhizobia for their plant growth promotion characteristics from the major growing areas of the country. In this study, groundnut rhizobia isolates were collected from major prospective groundnut growing areas of Ethiopia using groundnut variety Babile 1. The isolates were then evaluated for multiple plant growth promotion (PGP) traits under laboratory and greenhouse conditions to determine their potential and effectiveness for future inoculant production.

MATERIALS AND METHODS

Source of rhizobial isolates

A total of 72 groundnut rhizobia isolates were used for PGP tests. All of them were trapped by induction method under greenhouse condition from soil samples collected from major groundnut growing areas Oromia Babile, Benishangul and Berhet wereda by using improved groundnut variety called Babile 1 as a trap host. This variety was introduced from India by International Crop Research Semi-Arid and Tropics (IRISAT). It is well adapted in some areas of the country like that of Werer, Miesso, Assosa, Pawe and Babile with an altitude range between 569 to 1100 mm and having an average potential productivity of 24 qt/ha. The majority of isolates were slow growing rhizobia identified as *Bradyrhizobium* species.

Screening for plant growth promoting (PGP) characteristics of groundnut rhizobia

Solubilization of inorganic phosphates

A loopful of fresh rhizobial culture (10µL; 10^8 cells mL^{-1}) was spot inoculated on Pikovskay's medium containing Yeast Extract 0.5 Dextrose 10.0 Calcium Phosphate 5.0 Ammonium Sulphate 0.5 Potassium Chloride 0.2 Magnesium Sulphate 0.1 Manganese Sulphate 0.0001 Ferrous Sulphate 0.0001 Agar 15.0 (in g l^{-1} of distilled water): and incubated at 28-30°C for one week. Clear zone formation around the colonies was recorded as positive for inorganic phosphate solubilization. Phosphate solubilization index (the extent of phosphate solubilizing ability of bacterial isolates) was also determined (Paul and Sinha, 2017).

Phosphate Solubilization Index (SI) = B/A

Where; A = Colony diameter B = Total diameter (colony + halo zone)

Quantitative estimation of indole acetic acid (IAA) production

The ability of rhizobial isolates to produce indole acetic acid (IAA) was determined colorimetrically accordingly. The rhizobial cultures were grown at 28°C in YEM broth (containing K_2HPO_4 - 0.5 g, $MgSO_4$. $7H_2O$ - 0.2 g, NaCl - 0.1g Mannitol - 10.0 g Yeast extract 1 lit distilled water) supplemented with filter sterilized L-tryptophan (2 g l^{-1}) for 72 h on a shaker at 150 rpm, and centrifuged at 6,000 rpm for 15 min at 4ºC. 2 ml of the supernatant was mixed with 4 ml of Salkowski reagent (1 ml of 0.5M $FeCl_3$ solution in 50 ml of 35% perchloric acid) and the mixture was reserved at room temperature for 25 min in darkness. IAA production was confirmed due to the development of pink color. The intensity of pink color was read at 530 nm spectrophotometrically and the amount of IAA produced was extrapolated from the standard curve constructed from pure IAA (Loba Chemie) in the range of 5 to 100 µg/ml. Non-inoculated L-tryptophan supplemented YEM broth medium was used as control (Md Hoirul Azri, 2018).

Ammonia (NH3) production

The isolates were tested for ammonia production by inoculating a loopful of freshly grown cells in to 10 ml of pre-sterilized peptone water tubes and incubated at 28^0C for 3 days. The tubes were treated with 0.5 ml of Nessler's reagent (potassium iodide -50 g, saturated mercuric chloride -35 mL, distilled water -25 mL, potassium hydroxide (40%) -400 mL) to detect development of brown to yellow color as a positive test for ammonia production (Manasa et al., 2017).

Production of hydrogen cyanide (HCN)

The rhizobial isolates (100 µL; 10^8 cells mL^{-1}) were inoculated into

YEMA plates supplemented with 4.4 g L^{-1} of glycine to detect HCN production. Stripes of filter paper (Whatman filter paper No.1) were soaked in the yellow picric acid solution (2.5 g of picric acid and 12.5 g of Na_2CO_3 dissolved in 1L of distilled water) and fixed to the underside of the upper lids and sealed with parafilm (to avoid the escaping of volatiles like HCN) and incubated at 28°C for 5 days. A color change of the yellow filter paper to brown was recorded as positive for HCN production (Mir et al., 2021a).

In vitro antagonistic activity against test pathogenic fungus (Fusarium oxysporum)

The inhibitory effect of the rhizobia isolates against the pathogen, *F. oxysporum*, was evaluated *in vitro* on YEMA plates using the dual culture technique as described by Kumar et al. (2016). A loopful (10 µL; 10^8cells mL^{-1}) of each rhizobial culture was spot-inoculated on YEMA plates amended with 0.5% sucrose at a distance of 2.0 cm from the center at four equidistant points and incubated at 28°C for 5 days. Then, five days old mycelial discs (4 mm diameter) of *F. oxyporum* was positioned at the center of the Petri dishes and incubated at the same temperature until the test pathogen in the control plates (plates without rhizobia isolate) reached the edges of the plates. The radial growth of fungal mycelium and the inhibition percentage was compared with control using the formula, I = [C − T/C] × 100, where I is the percent inhibition and C and T are the pathogen radial growth in control and treatment, respectively.

Test for the production of different lytic enzymes

Cellulase production activity

Isolates were tested for their ability to produce cellulase according to the method. A loopful of broth culture (10 µL; 10^8 cells mL^{-1}) of each isolate was streaked on a cellulose agar media containing composition of KH_2PO_4 0.5 g, $MgSO_4$ 0.25 g, cellulose 2 g, agar 15 g, and gelatin 2 g; distilled water one liter and at pH 6.8–7.2. The plates were incubated at 28°C for 72 h and flooded with Gram's iodine for 5 min to detect clear zone formation around colonies (Dar et al., 2015).

Protease production activity

Protease activity was assayed with YEM agar containing 5% skimmed milk (Mohamad et al., 2018). After incubation at 28°C for 5–7 days, formation of clear halo zone around the bacterial colonies was positive reaction for milk casein hydrolysis.

Production of chitinase

Chitinase activity of the isolates was tested on chitin agar plates constituting (g l^{-1}) colloidal chitin (4), $MgSO_4.7H_2O$ (0.5), K_2HPO_4 (0.7), KH_2PO4 (0.3), $FeSO_4.7H_2O$ (0.01), $MnCl_2$ (0.001), NaCl (0.3), yeast extract (0.2) and agar (20). After adding iodine the development of clear zone around the colony was reflected as positive for the enzyme chitinase production (Madison et al., 2017).

RESULTS

Phosphate solubilizing ability of isolates

Phosphate-solubilizing bacteria were identified characteristically by the formation of a clear zone around the colonies after 48 h of incubation following spot inoculation in Pikovskaya's agar plate were taken as positive tests (Figure 1). Accordingly, out of the 72 rhizobial isolates, seventeen (17) isolates (23.6%) were capable of solubilizing tri-calcium phosphate. There was variation in the diameter of the halo zones surrounding each colony, indicating that these seventeen phosphate solubilizing bacteria exhibited differing capacities for phosphate solubilization (Table 1). The clear zone diameter ranged from 1 to 3 mm, with isolates GNR-67 and GNR-28, respectively. The phosphate solubilization indices formed by these isolates also varied between 1.7 and 2.45. The solublization index was calculated as: Phosphate Solubilization Index (SI) = B/A

Where; A = Colony diameter B = Total diameter (colony + halo zone)

Indole acetic acid (IAA) production

The isolates showed marked differences in their ability to produce IAA in tryptophan supplemented YEM broth media (Figure 2). Of the 72 isolates, 72% (52 isolates) produced a detectable amount of IAA, which ranged from 7.4 to 78.8 µg.ml^{-1}, while the auxin levels produced by the remaining 20 isolates were below the detection limit. A large amount of IAA was produced by isolate GNR-43 (78.8 µg.ml^{-1}) followed by isolates GNR-37 (77.2 µg.ml^{-1}), GNR-28 (67.8 µg.ml^{-1}), GNR-34 (66.8 µg.ml^{-1}), GNR-03 (65.8 µg.ml^{-1}), GNR-07 (58.8 µg.ml^{-1}) and GNR-54 (56.8 µg.ml^{-1}) (Table 1).

Ammonia (NH_3) production

Screening the rhizobial isolates for ammonia production was an important trait of plant growth-promoting rhizobacteria (PGPR) that indirectly influences plant growth and performance. Of all the tested Rhizobium isolates, two isolates were (GNR-28, GNR37) exhibited as strong (+++) ammonia producer, six isolates (GNR-3.GNR-7, GNR-19, GNR-34, GNR-43 and GNR-54) were produce moderately (++) .Whereas the rest isolates were scored as weak (+) for Ammonia production (Figure 3).

Antagonistic activity of *Rhizobium* against fungal pathogen

In vitro antagonistic potential of the *Rhizobium* isolates were tested against *F. oxysporum* in dual culture under *in vitro* conditions and the percentage of inhibition were recorded. After five days of incubation, inhibition zone was clearly visible. Hence, ten isolates were found to be inhibitory against fungal strain; yet, maximum inhibition potential was exhibited by the rhizobial isolates GNR-07

Figure 1. Clear zones of phosphate solublization for the isolates AAUR19, AAUR34 and AAUR37 on Pikovskaya's agar plate.

followed by GNR-03 and GNR-28 with growth inhibition of 42.3, 28 and 25.8% respectively against *F. oxysporum* (Table 1).

Production of different lytic enzymes

Screening of bacterial isolates for lytic enzymes production was done. Lytic enzymes include Protease, cellulase and chitinase positive isolates showed distinct, clear, and prominent zones of clearance around the colonies showing lytic enzymes production (Figure 4). In this study, of the tested isolates, 35 and 36 isolates showed positive for cellulase and protease activity, respectively. The majority (90%) of the isolates that produce cellulase enzyme also produce protease enzyme. However, all the tested isolates were negative for chitinase activity (data not shown).

Production of Hydrogen Cyanide (HCN)

HCN production is ascribed as one of the mechanisms of biocontrol activity of rhizobia, the ability of the 72 isolates to produce HCN was determined by the picric acid assay (Figure 5). Only two *Rhizobium* cultures, were produced HCN scored as moderate (++) for GNR-37 and weak for GNR-28 whereas the redcxw<nbvcxwdsfw<nbcw< sqmaining 70 isolates not changed the yellow color of the picric acid solution treated filter paper, implying majority of the groundnut isolate were failed to produce HCN (Table 1).

DISCUSSION

Among the tested rhizobial isolates, 17 (23.6%) isolates produce a halo zone around the colonies after 24 h of incubation on Pikovskaya's agar medium, which gradually increased up to 72h. The solubilisation efficiency (SE) of *Rhizobium* strains on solid media ranged between 71 to 150%. The *Rhizobium* strain GNR-28 showed maximum solubilisation efficiency followed by GNR-19 and GNR-34. In the study by Adnan et al. (2017), it was observed that 21% of the tested rhizobia were phosphate-solubilising bacteria, with solubilisation efficiencies ranging between 38 and 270%. Similarly, phosphate-solubilizing microorganisms Bacillus subtilis and Bacillus cereus, isolated by Satyanandam et al. (2021) from groundnut rhizosphere soil, exhibited maximum phosphate solubilizing zones. The isolates in the current study varied in their intrinsic ability to produce IAA as the production varied under the same condition. Hence, 72% of the tested isolates produced a detectable

Table 1. Summary of multiple plant growth promoting traits of groundnut rhizobial isolates.

Isolate	IAA produced	Phosphate solublization index	Ammonia Production	Protease	Cellulase	Chitinase	Antifungal activity	HCN	%PGP
GNR03	65.8	2.1	++	+	+	−	28	−	75
GNR05	8	NS	+	+	+	−	0	−	50
GNR08	32.5	2.21	+	−	+	−	12.3	−	40
GNR02	36	NS	+	+	−	−	0	−	37.5
GNR12	0	NS	+	+	+	−	0	−	37.5
GNR07	58.8	2.34	++	+	+	−	42.3	−	75
GNR15	23.4	NS	+	+	−	−	0	−	37.5
GNR17	0	NS	+	+	+	−	0	−	37.5
GNR19	76	2.42	++	+	+	−	22.5	−	75
GNR20	11.2	2.1	+	+	+	−	0	−	62.5
GNR24	32.2	2.24	+	+	+	−	0	−	62.5
GNR25	24.4	1.8	+	−	−	−	0	−	37.5
GNR26	0	NS	+	+	+	−	0	−	37.5
GNR27	0	NS	+	−	+	−	0	−	37.5
GNR28	67.8	2.45	+++	+	+	−	25.8	+	87.5
GNR29	32.4	2.33	+	+	−	−	0	−	50
GNR31	16.5	NS	+	−	+	−	0	−	37.5
GNR35	0	NS	+	+	+	−	12.3	−	50
GNR34	66.8	2.41	++	+	+	−	0	−	62.5
GNR36	28	NS	+	+	−	−	0	−	37.5
GNR37	77.2	2.4	+++	+	+	−	25	++	87.5
GNR38	11.6	NS	+	−	+	−	0	−	37.5
GNR42	42.4	1.8	+	+	−	−	0	−	50
GNR43	78.8	2	++	+	+	−	12.5	−	75
GNR44	33.4	NS	+	+	+	−	0	−	50
GNR46	7	NS	+	−	−	−	15.5	−	37.5
GNR47	33.7	2.22	+	−	+	−	0	−	50
GNR49	18.5	NS	+	+	+	−	0	−	50
GNR50	0	NS	+	+	+	−	0	−	37.5
GNR51	29.8	NS	+	−	+	−	0	−	37.5
GNR53	22	NS	+	+	−	−	0	−	37.5
GNR54	56.8	1.8	++	+	+	−	26.7	−	75
GNR55	0	NS	+	+	+	−	0	−	37.5
GNR58	34	2.31	+	−	+	−	0	−	50
GNR60	0	NS	+	+	+	−	0	−	37.5
GNR61	39.2	NS	+	+	−	−	0	−	37.5
GNR64	20.8	NS	+	+	+	−	0	−	50
GNR65	9.6	NS	+	−	+	−	0	−	37.5
GNR67	41.2	1.7	+	+	−	−	0	−	50
GNR68	7.4	NS	+	+	+	−	0	−	50
GNR71	34.8	1.74	+	+	+	−	0	−	62.5

amount of IAA, which ranged from 7.4 to 78.8 µg.ml^{-1}. The biosynthesis of IAA is widespread among plant-

Figure 2. IAA production of tested isolates AAUR37 (Pinkish color showed IAA production, Creamy color showed no IAA produced and Whitish color only YEM broth as control).

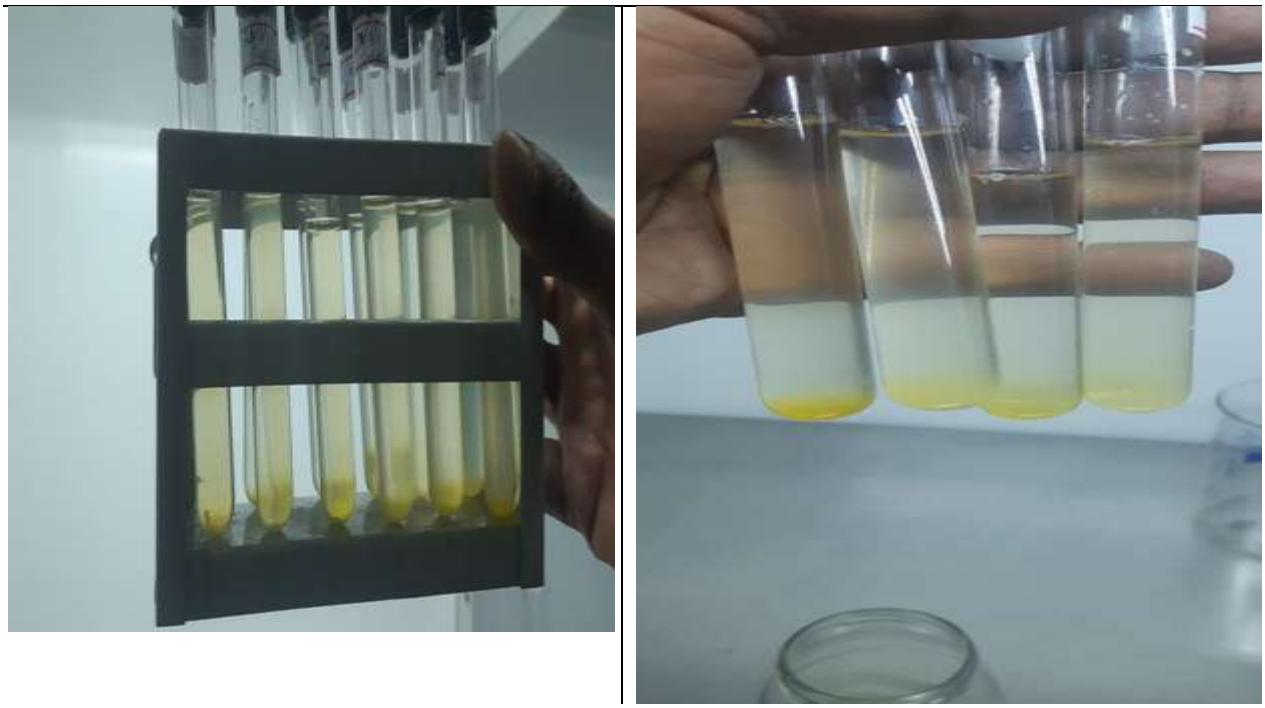

Figure 3..Test for ammonia production of rhizobial isolates AAUR19, AAUR28,AAUR37 and AAU43 from left to right(yellowish color indicates ammonium production).

associated bacteria (Ulrich et al., 2021). Several studies also showed that many soybean rhizobia produced IAA irrespective of the type of rhizobia nodulating groundnut host varieties (Dlamini et al., 2021; Ibny et al., 2019). Ibny et al. (2019) working with 89 rhizobial strains and found that 39% of the strains produce IAA. The IAA produced by some of the isolates in the present study was higher than previously reported for both fast and slow growing

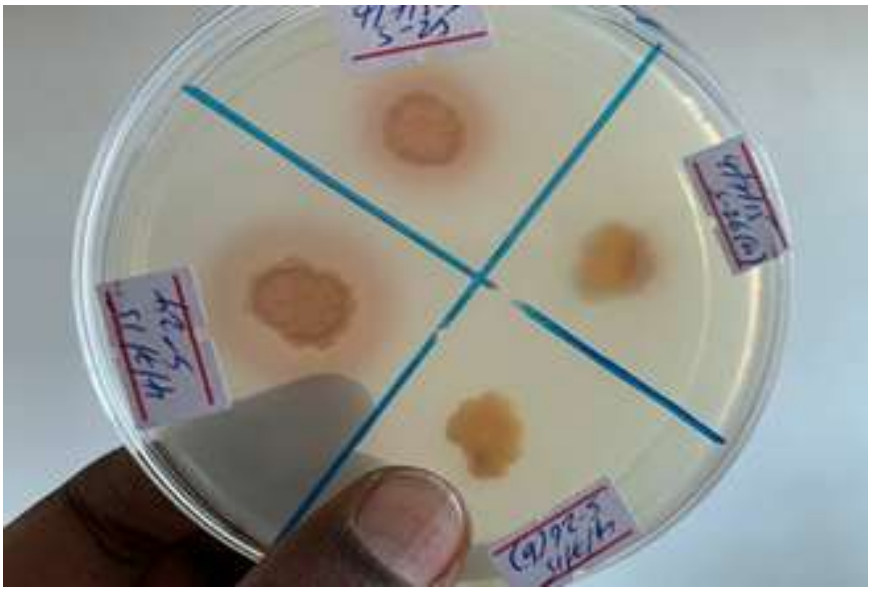

Figure 4. Protease enzyme production by rhizobial isolates AAUR19, AAUR28, and no protease production by isolates AAUR37and AAUR43 on SMA media.

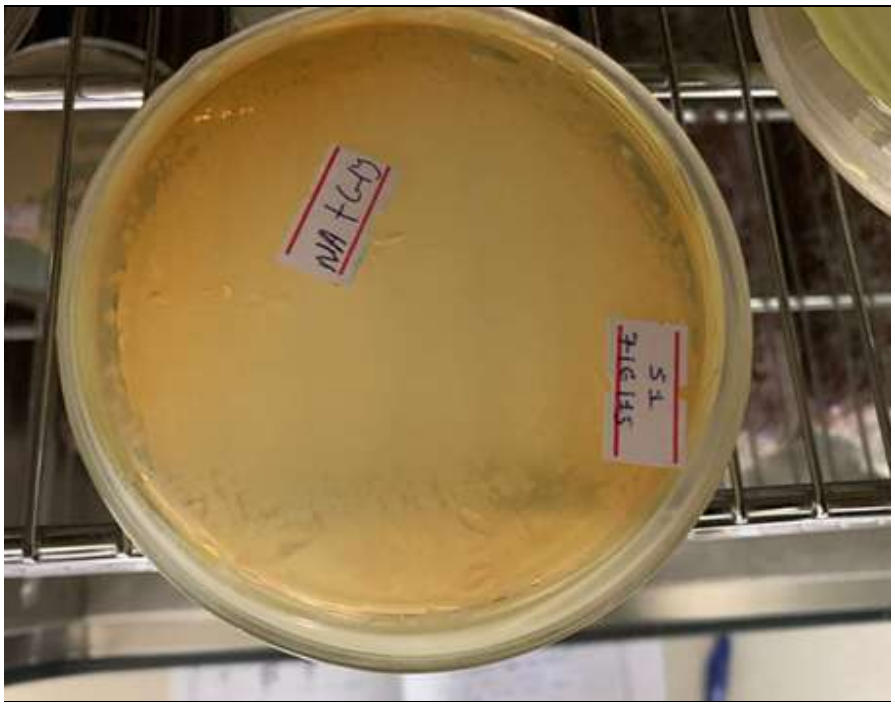

Figure 5. Plate based qualitative assays showing HCN production.

groundnut rhizobia in Pakistan (0.02 to 69.71 µg.ml−1). Ibny et al. (2019) and lower than which has been reported from Ghana (56 to 290 µg ml^{-1}) (Khalid et al., 2020). The production of IAA by PGPR can be differ with in species and strains, and influenced by culture conditions, substrate availability and growth stage (Ashrafuzzaman et al., 2009; Kumar et al., 2012; Ngoma et al., 2013).

Another important trait of rhizobia is the production of ammonia that indirectly influences the plant growth. The plants can take up ammonia produced by the rhizobia as a source of nitrogen for their growth. The ammonia

production results of the test isolates showed varied outcome (Table 1). All isolates (100%) were able to produce ammonia. Among these, two isolates were exhibited as strong ammonia producer, six isolates were produce moderately the remaining isolates were scored as weak ammonia producer. Similarly Ajilogba et al. (2022) works show that, even if all the tested isolates were positive for NH_3 production, two of them were recorded as moderate and the rest as weak ammonia producers. In general, having such rhizobia characteristics suggests that it is vital to select a nitrogen fixer with ammonia production in a bio-fertilizer consortium for agriculture practices.

To check the efficacy of antagonism of selected rhizobial isolates against soil borne fungal isolates (*F. oxysporum*) infecting groundnut plant, dual culture method was adapted and the percentage of inhibition of growth was recorded (Table 1). As a result of the plate assay, some rhizobial isolates curtailed the growth of pathogenic fungi tested and were found to be highly inhibitory to *F. oxysporum,* whereas other strains showed only nominal antifungal activity. Rhizobial Strains GNR-07, GNR-03 and GNR-28 suppressed the growth of tested fungi at higher percentage when compared to other strains tested. Similar results were observed by Antoun et al. (1998), who found that 49 of his rhizobial strains inhibited the growth of *F. oxysporum*. A significant reduction in damping -off or wilt disease of groundnut plant could be achieved by inoculating the strains that have antifungal ability and capable to reduce the percentage of crop loss. Such biocontrol agents have also been reported to produce toxic metabolites, enzymes or volatile compounds that have inhibitory effects on soil-borne pathogens.

Hydrolytic enzymes act as agents for prevention of plant diseases by causing lysis of pathogenic microbes in the close vicinity of the plant as they secrete increased level of cell wall lytic enzymes (Protease, cellulase and chitinase) (Neeraja et al., 2010). In this study, 50% isolates were positive for protease production and 48% isolates were positive for cellulase enzyme production. Even if there is no work on groundnut rhizobia in production of different lytic enzymes in Ethiopia, similar result reported by Abera et al. (2018) that indicate 33 and 38% of soybean rhizobia isolated from Ethiopian soils showed protease and cellulase activity, respectively whereas, none of them utilized chitin. PGPR that able to produce these lytic enzymes are expected to have biocontrol property against a wide range of fungi and bacteria that are potentially pathogenic for the plant and led the crop to enhance crop yield.

Bacterial isolates for their production ability of hydrogen cyanide (HCN) was also screened. Of all the tested *Rhizobium* isolates (72) for Hydrogen Cyanide, only two isolates showed moderate and weak production (Table 1).

Irrespective of the types of host plants, out of 22-tested soybean isolates which isolated from Ethiopia soil only one isolate produced HCN (Getahun et al., 2022). Earlier, Antoun et al. (1998) have also reported that only 3% of rhizobial strains from different genera and species were found to produce HCN, implying the rare occurrence of HCN production among rhizobia species, indicating that PGP rhizobia are relatively inefficient in the production HCN (Mir et al., 2021b).

In general, presence or absence and intensity of Hydrogen Cyanide production can play a significant role in antagonistic potential of bacteria against phytopathogens.

Conclusion

The current study covers the way for the ideal selection of *Rhizobium* possessing multiple PGPR properties and confirmed antagonistic activity for their consistent performance on the growth and yield of groundnut. Selection of the appropriate rhizobial inoculant improves nitrogen fixation and food production. The present study was mainly taken up to screen and identify multiple PGPR trait producers of rhizobial isolates isolated from the major groundnut growing area of the country and to use it as a biofertilizer for stimulating the growth of groundnut. The ability of tested *Rhizobium* isolates exhibiting some PGP-properties, namely, IAA production, PSB, ammonia, HCN, lytic enzyme (protease, cellulase and chitinase) production and antagonistic activity evaluated under in vitro conditions. Accordingly, isolates such as GNR-37 and GNR-28 proved 85% efficiency followed by GNR-43, GNR-19 and GNR-which showed 75% efficiency performance from the all tested traits. Owing to this, the isolates that showed much multiple traits have a selective advantage for practical application to formulate an inoculant for groundnut.

ACKNOWLEDGEMENTS

The authors are thankful to the scientific support of Applied microbiology Labortory and Department of MCMB, Addis Abeba University, and Menagesha Biotech Industry, Ethiopia.

CONFLICT OF INTERESTS

The authors have not declared any conflict of interests.

REFERENCES

Abera Y, Masso C, Assefa F (2018). Phenotypic, Host Range and Symbiotic. Ethiopian Journal of Agricultural Sciences 28(3):95-116.

Adnan M, Shah Z, Fahad S, Arif M, Alam M, Khan IA, Mian IA, Basir A, Ullah H, Arshad M (2017). Phosphate-solubilizing bacteria nullify the antagonistic effect of soil calcification on bioavailability of phosphorus in alkaline soils. Scientific Reports 7(1):16131.

Afzal A, ZAsad SA (2019). Microbial Applications for Sustainable

Agriculture. Innovations in Sustainable Agriculture, pp. 43-77.
Ajilogba CF, Babalola OO, Adebola P, Adeleke R (2022). Bambara Groundnut Rhizobacteria Antimicrobial and Biofertilization Potential. Frontiers in Plant Science 13:854937. doi: 10.3389/fpls.2022.854937.
Antoun H, Beauchamp CJ, Goussard N, Chabot R, Lalande R (1998). Potential of Rhizobium and Bradyrhizobium species as plant growth promoting rhizobacteria on non-legumes: effect on radishes (Raphanus sativus L.). Molecular microbial ecology of the soil: results from an FAO/IAEA co-ordinated research programme, 1992–1996, pp. 57-67.
Ashrafuzzaman M, Hossen FA, Ismail MR, Hoque A, Islam MZ, Shahidullah S, Meon S (2009). Efficiency of plant growth-promoting rhizobacteria (PGPR) for the enhancement of rice growth. African Journal of Biotechnology 8(7).
Dar MA, Pawar KD, Jadhav JP, Pandit RS (2015). Isolation of cellulolytic bacteria from the gastro-intestinal tract of Achatina fulica (Gastropoda: Pulmonata) and their evaluation for cellulose biodegradation. International Biodeterioration and Biodegradation 98:73-80.
Dlamini ST, Jaiswa, SK, Mohammed M, Dakora FD (2021). Studies of phylogeny, symbiotic functioning and ecological traits of indigenous microsymbionts nodulating Bambara groundnut (*Vigna subterranea* L. Verdc) in Eswatini. Microbial Ecology 82(3).
Getahun A, Muleta D, Assefa F, Kiros S, Hungria M (2022). Phytobeneficial traits of Rhizobacteria isolated from degraded soil and evaluate their effect in augmentation of Acacia (*Acacia abyssinica* Hochst. Ex Benth) seeds germination. SINET: Ethiopian Journal of Science 45(3):330-346.
Gopalakrishnan S, Sathya A, Vijayabharathi R, Varshney RK, Gowda CL, Krishnamurthy L (2015). Plant growth promoting rhizobia: challenges and opportunities. 3 Biotech 5:355-377.
Hamid S, Lone R, Mohamed HI (2021). Production of antibiotics from PGPR and their role in biocontrol of plant diseases. Plant Growth-promoting Microbes For Sustainable Biotic and Abiotic Stress Management pp. 441-461.
Ibny FY, Jaiswal SK, Mohammed M, Dakora FD (2019). Symbiotic effectiveness and ecologically adaptive traits of native rhizobial symbionts of Bambara groundnut (*Vigna subterranea* L. Verdc.) in Africa and their relationship with phylogeny. Scientific Reports 9(1):1-17.
Jaiswal SK, Mohammed M, Ibny FY, Dakora FD (2021). Rhizobia as a source of plant growth-promoting molecules: Potential applications and possible operational mechanisms. Frontiers in Sustainable Food Systems 4:619676.
Jayaprakashvel M, Chitra C, Mathivanan N (2019). Metabolites of plant growth-promoting rhizobacteria for the management of soilborne pathogenic fungi in crops. Secondary Metabolites of Plant Growth Promoting Rhizomicroorganisms: Discovery and Applications pp. 293-315.
Jha CK, Saraf M (2015). Plant growth promoting rhizobacteria (PGPR): a review. Journal of Agricultural Research and Development 5(2):108-119.
Kaur R, Kaur S, Kaur N (2021). Phosphate solubilizing bacteria: a neglected bioresource for ameliorating biotic stress in plants. In Plant-microbe dynamics: recent advances for sustainable agriculture. CRC Press. pp. 39-50
Khalid R, Zhang XX, Hayat R, Ahmed M (2020). Molecular characteristics of rhizobia isolated from Arachis hypogaea grown under stress environment. Sustainability 12(15): 6259.
Knežević M, Buntić A, Delić D, Stajković-Srbinović O (2022). Root Nodule Bacteria-Rhizobia: Exploring the Beneficial Effects on Non-legume Plant Growth. In Nitrogen Fixing Bacteria: Sustainable Growth of Non-legumes. Springer pp. 129-168.
Kumar A, Kumar A, Devi S, Patil S, Payal C, Negi S (2012). Isolation, screening and characterization of bacteria from Rhizospheric soils for different plant growth promotion (PGP) activities: an in vitro study. Recent Research in Science and Technology 4(1):1-5.
Kumar P, Pandey P, Dubey RC, Maheshwari DK (2016). Bacteria consortium optimization improves nutrient uptake, nodulation, disease suppression and growth of the common bean (*Phaseolus vulgaris*) in both pot and field studies. Rhizosphere 2:13-23.
Kumar V, Kayasth M, Chaudhary V, Gera R (2014). Diversity of diazotrophs in arid and semi-arid regions of Haryana and evaluation of their plant growth promoting potential on Bt-cotton and pearl millet. Annals of Microbiology 64:1301-1313.
Madison JD, Berg EA, Abarca JG, Whitfield SM, Gorbatenko O, Pinto A, Kerby JL (2017). Characterization of *Batrachochytrium dendrobatidis* inhibiting bacteria from amphibian populations in Costa Rica. Frontiers in Microbiology 8:290.
Manasa K, Reddy S, Triveni S (2017). Characterization of potential PGPR and antagonistic activities of Rhizobium isolates from different rhizosphere soils. Journal of Pharmacognosy and Phytochemistry 6(3):51-54.
Md Hoirul Azri P (2018). Effects of Bacillus salmalaya strain 139SI on oil palm *(Elaeis guineensis Jacq.)* growth and yield/Md Hoirul Azri Ponari Universiti Malaya].
Meena B, Altaf MM, Ahmad I (2012). Functional diversity of indigenous plant growth promoting rhizobacteria (PGPR) isolated from Aligarh soils. Advances in Life Sciences 1:58-61.
Mir MI, Kumar BK, Gopalakrishnan S, Vadlamudi S, Hameeda B (2021a). Characterization of rhizobia isolated from leguminous plants and their impact on the growth of ICCV 2 variety of chickpea (*Cicer arietinum* L.). Heliyon 7(11):e08321.
Mir MI, Kumar BK, Gopalakrishnan S, Vadlamudi S, Hameeda B (2021b). Characterization of rhizobia isolated from leguminous plants and their impact on the growth of ICCV 2 variety of chickpea (*Cicer arietinum* L.). Heliyon 7(11).
Mohamad OA, Li L, Ma JB, Hatab S, Xu L, Guo JW, Rasulov BA, Liu YH, Hedlund BP, Li WJ (2018). Evaluation of the antimicrobial activity of endophytic bacterial populations from Chinese traditional medicinal plant licorice and characterization of the bioactive secondary metabolites produced by Bacillus atrophaeus against Verticillium dahliae. Frontiers in Microbiology 9:924.
Moustaine M, Elkahkahi R, Benbouazza A, Benkirane R, Achbani E (2017). Effect of plant growth promoting rhizobacterial (PGPR) inoculation on growth in tomato (*Solanum Lycopersicum* L.) and characterization for direct PGP abilities in Morocco. International Journal of Environment, Agriculture and Biotechnology 2(2):238708.
Neeraja C, Anil K, Purushotham P, Suma K, Sarma P, Moerschbacher BM, Podile AR (2010). Biotechnological approaches to develop bacterial chitinases as a bioshield against fungal diseases of plants. Critical Reviews in Biotechnology 30(3):231-241.
Ngoma L, Esau B, Babalola OO (2013). Isolation and characterization of beneficial indigenous endophytic bacteria for plant growth promoting activity in Molelwane Farm, Mafikeng, South Africa. African Journal of Biotechnology 12(26).
Olanrewaju OS, Glick BR, Babalola OO (2017). Mechanisms of action of plant growth promoting bacteria. World Journal of Microbiology and Biotechnology 33:1-16.
Panigrahi S, Mohanty S, Rath C (2020). Characterization of endophytic bacteria Enterobacter cloacae MG00145 isolated from Ocimum sanctum with Indole Acetic Acid (IAA) production and plant growth promoting capabilities against selected crops. South African Journal of Botany 134:17-26.
Paul D, Sinha SN (2017). Isolation and characterization of phosphate solubilizing bacterium Pseudomonas aeruginosa KUPSB12 with antibacterial potential from river Ganga, India. Annals of Agrarian Science 15(1):130-136.
Sathya A, Vijayabharathi R, Gopalakrishnan S (2017). Plant growth-promoting actinobacteria: a new strategy for enhancing sustainable production and protection of grain legumes. 3 Biotech 7:1-10.
Satyanandam T, Babu K, Suneeta D, Bhaskararao C, Rosaiah G, Vijayalakshmi M (2021). Isolation and Screening of Indigenous Rhizobia from BlackGram Cultivated in Fallow Rice Soils for Plant Growth Promoting Traits. Malaysian Journal of Soil Science P 25.
Ulrich K, Kube M, Becker R, Schneck V, Ulrich A (2021). Genomic analysis of the endophytic Stenotrophomonas strain 169 reveals features related to plant-growth promotion and stress tolerance. Frontiers in Microbiology 12:687463.
Vargas LK, Volpiano CG, Lisboa BB, Giongo A, Beneduzi A, Passaglia LMP (2017). Potential of rhizobia as plant growth-promoting rhizobacteria. Springer.

Vol. 17(9), pp. 221-229, September 2023
DOI: 10.5897/AJMR2023.9712
Article Number: 8141F5671263
ISSN: 1996-0808
Copyright©2023
Author(s) retain the copyright of this article
http://www.academicjournals.org/AJMR

ACADEMIC JOURNALS
expand your knowledge

African Journal of Microbiology Research

Full Length Research Paper

Density and diversity of arbuscular mycorrhizal fungi in *Anacardium occidentale* L. plantations in Senegal

Khémes Marie Odile THIOCONE[1]*, Abdoulaye SOUMARE[1], Mohamed Mahamoud CHARAHABIL[1], Landing NDIAYE[1], Fatou NDOYE[2], Saliou FALL[3], Valérie HOCHER[4] and B. A. AMADOU[5]

[1]Department of Agroforestry, Assane Seck University of Ziginchor, Senegal.
[2]Agronomy and Plant Production Department, University of Sine Saloum of Kaolack El Hadj Ibrahima Niass, Senegal.
[3]Joint Microbiology Laboratory, Sénégal.
[4]Research Institute for Development, Montpellier, France.
[5]University of the West Indies, Guadeloupe, France.

Received 4 July, 2023; Accepted 4 September, 2023

Cashew nut cultivation plays an important socio-economic role in Senegal. However, it suffers from several problems, including declining soil fertility which leads to low productivity. To overcome these constraints, the use of arbuscular mycorrhizal fungi (AMF) could be a sustainable alternative. However, the positive effects of AMFs may depend on their infectious potential, density, and diversity. So far, little attention has been given to exploring these aspects in cashew plantations. The proposal of this study is to determine the infectious propagules, density and diversity of AMF spores in cashew agro-systems. Soil samples were collected from four cashew production areas in Senegal (Ziguinchor, Sédhiou, Kolda and Fatick). The soil samples were previously treated by wet sieving and decantation technique and the spores were isolated by centrifugation; thereafter, a morphological identification of the extracted spores was carried out. To compare AMF propagule numbers between sites, a most probable number (MPN) bioassay was performed under greenhouse conditions using *Zea mays* as the host plant. The average AMF spore density was significantly higher in Ziguinchor (610 spores/100 g soil), Sédhiou (586 spores/100 g soil), and Fatick (445 spores/100 g soil) compared to Kolda (211 spores/100 g soil). However, no significant difference was noted between Ziguinchor, Sédhiou, and Fatick. Spore and propagule densities show opposite results, MPN was high in sites with low spore density. The identification of the spores showed 6 genera belonging to *Glomus*, *Gigaspora*, *Acaulospora*, *Scutellospora*, *Entrophospora,* and Racocetra. Identified AMFs could be isolated and multiplied to produce bioinoculants for cashew trees.

Key words: Abundance, Arbuscular mycorrhizal fungi, morphological diversity, most probable number, *Anacardium occidentale,* Senegal.

INTRODUCTION

Cashew is a tropical nut crop and an extremely important source of income for thousands of people in Senegal. It is cultivated widely in the South of the country, especially in Casamance and in the Groundnut Basin of Senegal with a national production estimated at around 28 900 tons per year (Hien, 2019). In Casamance, cashew is mainly grown in the administrative regions of Kolda, Sedhiou, and Ziguinchor, while in the Groundnut Basin it concerns

the Factick region. Cashew constitutes a major source of income in these regions by supporting more than 22500 households which represent a total population of around 352600 inhabitants (ASEPEX and IRD, 2017). In spite of the importance of this crop, cashew nuts yields gradually declined during these past years (Ndiaye et al., 2017). Currently, the yield per tree fluctuates from 3.2 to 5.81 kg and the yield per hectare is around 542 kg/h (Samb et al., 2018b). This production remains low compared to other producing countries such as Brazil, Vietnam, India, Indonesia, Philippines, Ivory Coast, Nigeria, and Benin (Samb et al., 2018b). Of the several factors associated with low productivity, poor soil fertility especially in nitrogen and phosphorus is a major factor limiting production. In addition, very little attention, in term of research has been accorded to this crop. There is therefore the need to step up research to improve cashew production, yields and quality as well as standardize effective propagation techniques to increase the productivity of this crop. In this context, the use of Abuscular Mycorrhizal Fungi (AMF) could promote plant growth and provide protection against phytopathogens (Sadhana, 2014; Barrow, 2012). In fact, under natural conditions, plants maintain symbiotic relationships with microorganisms as a strategy to withstand adversities by increasing plant resilience to water deficit and soil nutrient scarcity (Cius, 2017; Manga et al., 2022; Soumare et al., 2023). So, it is important to know which AMF are present in rhizosphere and in roots of naturally occurring plants in order to identify the most frequent ones and those showing high adaptability to environmental conditions. In fact, variations in AMF diversity can influence the stability and population dynamics of an ecosystem by changing plant competiveness and persistence. However, until recently, there was little focus on AM fungal diversity and ecosystem variability and productivity. This study aims to assess the MPN of infective propagules, density and diversity of AMF associated to *Anacardium occidentale* L. in different cashew agro-ecological zones in Senegal.

MATERIALS AND METHODS

Presentation of the study area

This study was conducted in two agro-ecological zones: the Casamance and the Groundnut Basin favorable to cashew cultivation (Figure 1). In Casamance, the sampling sites corresponding to the administrative regions of Kolda (Sanankoro 12°53'00" N, 14°57'00" W), Sédhiou (Colane 12°42'29" N, 15°33 '25" W) and Ziguinchor (Boutoupa Camaracounda 12°33'40" N, 16°17'00" W) while in groundnut Basin, the sampling have been taken in Fatick region (Ndiémou 14°19'00" N, 16°25'00 " O).

In Casamance, the annual rainfall varies between 600 and 1775 mm distributed from June to October with an annual average temperature of 26.7°C (Camara, 2018). The soils are tropical ferruginous and/or ferralitic, clayey-loamy, hydromorphic types (ANSD, 2013). By contrast, Fatick region belongs to semi-arid tropical climate with an average annual temperature between 21 and 37°C and an average annual rainfall of 611 mm (Samb et al., 2018a). The soils are saline and acidified saline halomorphic soils (Samb et al., 2018a).

Soil sampling

At each site, five composite soil samples were obtained from under five *A. occidentale* trees. The sampling was carried out at a distance of 3/4 of the crown radius at a soil depth of 0 to 20 cm, following the East, West, North, and South directions of each tree. The soils that have been taken from each tree are mixed together to form a composite sample. Five composite samples were collected per site.

Characterization physicochemical of soils

A physical and chemical characterization of the soil was carried out in the Laboratory of Soil, Water and Plant of ISRA/CNRA in Bambey following the method of Bremner and Mulvaney (1982). The samples were placed in a mechanical shaker and sieved for 5 min through a series of sieves with 50, 100, 250, 500, and 1000 µm diameter to determine the size of different soil particles. All soil samples were characterized by measuring pH, total soil C and N after dry combustion in Elemental Analyzer (LECO Corporation, St. Joseph, MI, USA). Total and available P were analyzed by Olsen-Dabin method (Aubert, 1978). Other components were also determined such as Ca^{2+}, Mg^{2+}, and K^{+} the Atomic Absorption Spectrophotometry method and exchangeable aluminium was used (David, 1960).

Quantification and taxonomic identification of AM fungi spores

For each composite sample, the AM fungi spores were isolated from *A. occidentale* rhizosphere by using a wet sieving and decanting technique according to Gerdemann and Nicolson (1963). Three subsamples (100 g) from each sample were independently suspended in 500 mL of water in a beaker. After the settlement of heavier particles, the suspension was carefully poured on a stack of sieves (500, 200, 100 and 50 µm, arranged µm mesh size) arranged in descending order. The processes were repeated almost three times to trap all spores of AM fungi. The AM fungal spores on the bottom sieves, to know, 100 and 50 µm, were collected. Spores were purified by re-suspending the sieving in 60% of sucrose solution and centrifuged at 1000 rpm for 5 min at 4°C. Afterwards, the AM fungal spores were rinsed in tap water and were counted under a microscope. Result was expressed as the spore number per 100 g of dry.

The AM spores of different genera have been described by spore morphology and as per the standard key referring to Souza (2015) and the INVAM (https://invam.ku.edu/spores). The identification of each spore type was done on the basis of color, shape, size, surface ornamentation, spore wall structure and type of hyphal attachment (Redecker et al., 2013). Identification of AM spores was done after trap culturing as propagation of field collected AM

*Corresponding author. E-mail: k.thiocone5328@zig.univ.sn. Tel: +221773863152.

Author(s) agree that this article remain permanently open access under the terms of the Creative Commons Attribution License 4.0 International License

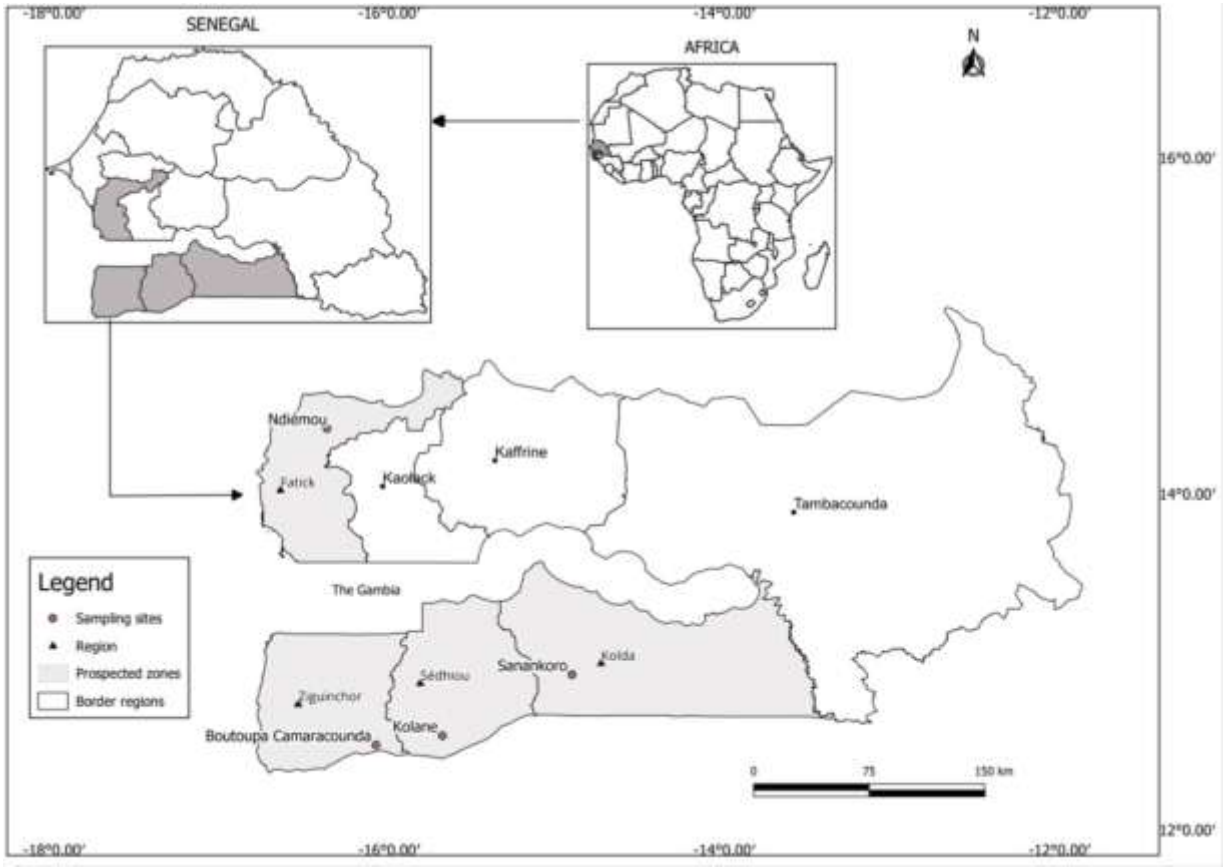

Figure 1. Map of Senegal indicating the culture area of cashew in Senegal and the soils sampling zone.

species sometimes require controlled environment.

The most probable number (MPN) of AM fungi

This has been used to determine total propagules based on colonization of roots of the assay host. MPN is based on the use of a series of successive soil dilutions form 10^{-1} to 10^{-6} (Mosse, 1986). The dilutions were prepared by mixing the original soil with the same soil autoclaved at 120°C for 1 h (Gianinazzi and Vosátka, 2004). The soil mixture is divided into five replicates of 50 g/pot. One pregerminated *Zea mays* seeds were planted per pot under greenhouse conditions. After 45 days, the plants were uprooted and root system was stained according to the method of Phillips and Hayman (1970) in order to visualize the structures' mycorrhizal. Using non mycorrhized and mycorrhized roots obtained for each level of dilutions, the MPN of propagules present in soil was calculated with the formula of Fisher and Yates (1963):

log = (x × log a) − K, which is the estimated number of propagules;

where 'x' is the mean of positive pots; 'a' is the dilution factor and 'K' is a constant on Fisher and Yates' statistical. Results were expressed as number of propagules per unit soil.

Data analysis

All the data obtained were entered using the spreadsheet excel version 2013. The data were statistically analyzed using the XLSTAT software version 2016. A comparison between the treatments was carried out using an analysis of one-way variance (ANOVA). Significant differences between spore abundance and between soil physical and chemical properties were tested using Fisher's least significant difference (LSD) for $P < 0.05$. A principal component analysis (PCA) was used to determine the multiple correlations between the physicochemical properties of the soils and the types of AMF identified in the sampling sites. Some data were previously transformed by the formula Arsin√ x to normalize them. The MPN of arbuscular mycorrhizal fungi was calculated using the excel table.

RESULTS

Physico-chemical soil analysis

The grain size analysis and the soil texture triangle showed a textural variability of soils between the two agro-ecological zones. The soils sampled from the three areas of the agro-ecological zone of Casamance (Ziguinchor, Kolda and Sedhiou) are clays sand, while the soil of the agro-ecological zone of Groundnut Basin (Fatick) is sandy. The analysis of soils' chemical parameters revealed a significant difference (p-value <0.05) in their content in nitrogen, Ca^{2+} cation, and pH

Table 1. Physico-chemical characteristics of soils.

Physicochemical property	Localities			
	Ziguinchor	Sédhiou	Kolda	Fatick
Physical				
Sands (%)	87.64^{b}	86.48^{b}	89.77^{ab}	94.82^{a}
Stringers (%)	4.814^{a}	5.67^{a}	5.49^{a}	2.81^{ab}
Clays (%)	7.546^{a}	7.86^{a}	4.75^{ab}	2.38^{b}
Chemical				
pH	5.11^{b}	5.18^{b}	5.41^{b}	6.07^{a}
C (%)	0.514^{a}	0.71^{a}	0.48^{a}	0.63^{a}
N (%)	0.056^{b}	0.05^{b}	0.04^{b}	0.09^{a}
MO (%)	0.886^{a}	1.22^{a}	0.84^{a}	1.08^{a}
C/N	9.542^{ab}	14.08^{a}	12.63^{ab}	6.78^{b}
P (ppm)	11.877^{a}	9.73^{a}	8.71^{a}	14.74^{a}
Ca^{2+}	1.829^{a}	1.87^{a}	2.20^{a}	0.64^{b}
Mg^{2+}	0.22^{b}	0.29^{ab}	0.25^{ab}	0.46^{a}
K^{+}	0.072^{a}	0.07^{a}	0.08^{a}	0.13^{a}

In the same line, the values followed by the same letter are not significantly different at 5% threshold according to the Newman-Keuls test. pH: potential of the hydronium ion, C%: proportion of total organic carbon, N%: proportion of total nitrogen, C/N: the ratio between proportion of total organic carbon and proportion of total nitrogen, OM%: the organic matter content, P. assimilable: assimilable phosphorus, Ca^{2+}: calcium ion, Mg^{2+}: magnesium, K^{+}: the potassium ion.

values (Table 1). The soils pH of Casamance agro-ecological areas is slightly acidic and show similar values in the three sites. These soils are also characterized by low values of N (%) and high value of Ca^{2+} elements. However, the soils from Fatick agro-ecological were less acidic and closer to neutral pH (6). The soils as opposed to Casamance soils are characterized by high values of N (%), lowest Ca^{2+} cation content, and C/N ratio.

However, no significant differences (p-value >0.05) were observed in organic carbon matter, assimilable phosphorus, and K^{+} cation, between sampling sites.

Density of AMF spores in the different sites studied

The results indicate a variation of the density of the spores according to the sites (Figure 2). The density is significantly higher in Ziguinchor (610 spores/100 g of soil), Sédhiou (445 spores/100 g of soil) and Fatick (445 spores/100 g of soil) compared to Kolda (211 spores/100 g of soil). Variance analysis did not show significant (P >.0. 05) difference in the number of spores between Ziguinchor, Sédhiou and Fatick sites. However, the latter were significantly lower in Kolda.

Morphological diversity of arbuscular mycorrhizal fungi

Six genera of AMF morphotypes were recorded from the different sites based on morpho-anatomical features of the spores (Figure 3). The observed genera are *Glomus*, *Gigaspora*, *Racocetra*, *Entrophospora*, *Scutellospora* and *Acaulospora*. These genera belong to Glomerales and Diversisporales orders.

The analysis of variance shows that the genera *Glomus* showed significantly the highest frequencies (66.75%) followed by *Acaulospora* (23.87%), while *Gigaspora, Scutellospora, Entrophospora* and *Racocetra* genera recorded the lowest frequencies (4.8, 2.17, 1.52, and 0.87% respectively). In addition, there were no significant differences between these genera

AMF spore abundance according to the different sites

The analysis of variance (Table 2) revealed that the genera of *Scutellospora*, *Glomus*, *Gigaspora*, and *Entrophospora* have a significantly different abundance depending on the sites. However, the genera of *Acaulospora* and *Racocetra* do not show any significant difference between sites.

Abundance of AMFs infective propagules (MPN)

The number of infective propagules of the different site is presented in Table 3. This number varied between from the lowest mean value of 141. 6 recorded in Ziguinchor and to the highest mean value of 992.05 recorded in Fatick and Kolda. The MPN of infective propagules in 100

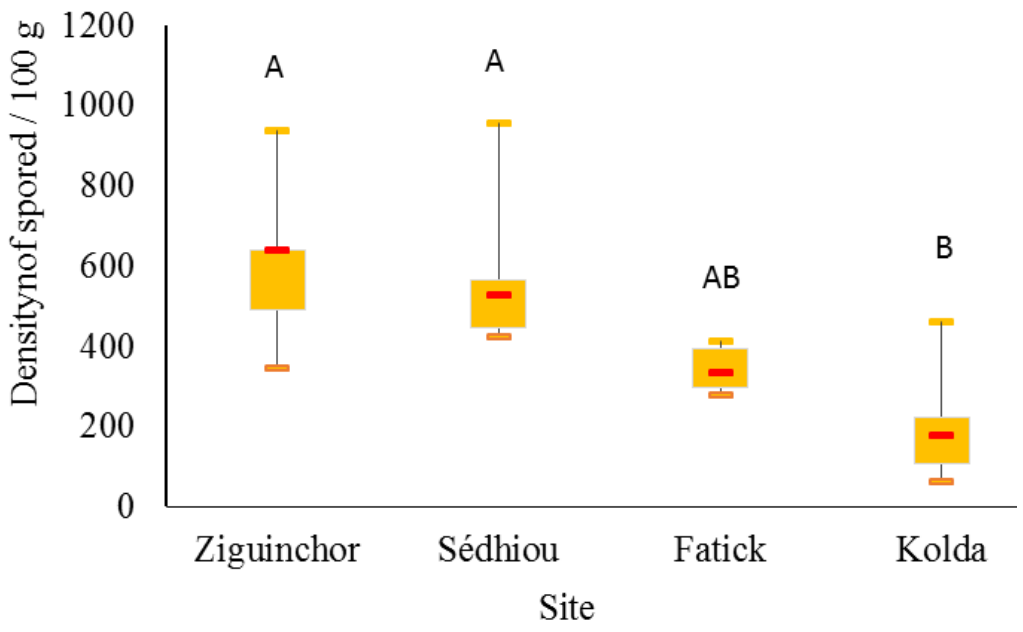

Figure 2. AMF spore abundance according to sites. The values followed by the same letter are not significantly different at the 5% level according to the Fisher test.

Table 2. Distribution of AMFs isolated from soils of cashew sites.

Site	Gender						
	Scutellospora	***Acaulospora***	***Racocetra***	***Glomus***	***Gigaspora***	***Entrophospora***	**Total abundance**
Fatick	22^{a}	48^{a}	8^{a}	267^{ab}	62^{a}	21^{a}	344^{ab}
Sédhiou	6^{b}	100^{a}	4^{a}	456^{a}	17^{ab}	4^{a}	565^{a}
Ziguinchor	4^{b}	131^{a}	1^{a}	469^{a}	4^{b}	2^{a}	604^{a}
Kolda	4^{b}	97^{a}	2^{a}	105^{b}	3^{b}	1^{a}	208^{b}
Pr > F	0.00	0.32	0.13	0.002	0.013	0.044	0.007
Significant	Yes	No	No	Yes	Yes	Yes	Yes

The values followed by the same letter are not significantly different at the 5% level according to the Fisher test.

g of dry soil for Sédhiou was 524.95 propagules/100 g of dry soil.

Relationship between soil physico-chemical properties and AMF spores abundance

Figure 4 presents the correlation between the abundance of AMF spores and the physicochemical properties of soils. The contribution of axis F1 is 74.15% collecting *Gigaspora*, *Scutellospora*, *Entrophospora* and *Racocetra.* This axis is related to high total N and assimulable P and characterize Fatick site which is opposed to the site of Ziguinchor. The axis 2 account for 16.67% and is related to high C% and MO% content in soil and abundance of *Glomus* characterize Sédhiou site which is opposed to Kolda site and that of axis 2 is 16.67%.

Analysis of Table 4 shows that there is a positive correlation between spore abundance and available phosphorus, carbon, nitrogen and organic matter. On the other hand, a negative correlation was observed between the abundance of spores and the pH, but also between the abundance of spores and the C/N ratio. It was also noted that the MPN of the soils studied are positively correlated with pH, phosphorus, carbon, nitrogen and organic matter.

DISCUSSION

The abundance of morphotype spores (spore density) and MPN estimates of AMF infective propagules were significantly variable depending on the exploited site. Our results showed that soil properties played important roles

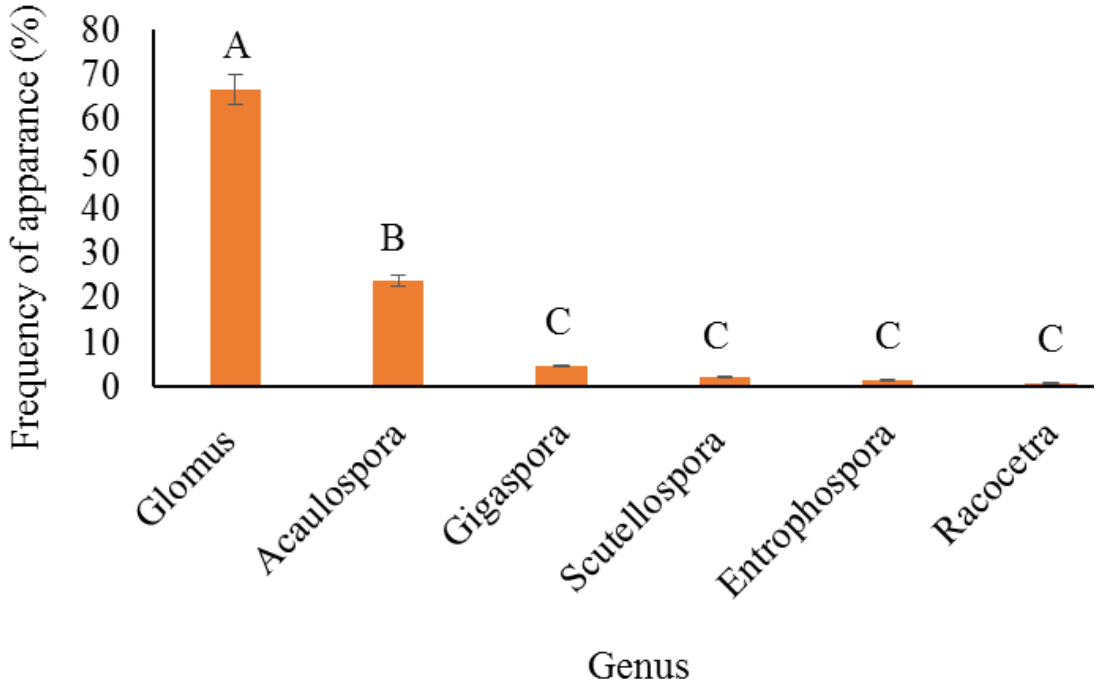

Figure 3. Frequency of appearance of spores according to genera. The values followed by the same letter are not significantly different at the 5% level according to the Fisher test.

Table 3. Most probable number of propagules in 100 g of dry soil from each site.

Feature	Sites			
	Ziguinchor	**Kolda**	**Sédhiou**	**Fatick**
Number of propagules/100 g of dry soil	141.60	992.05	524.95	992.05
Confidence interval at the threshold of P<5%	302.59< 141.60 < 62.26	2119.97< 992.05 < 464.23	1121.80< 524.95 < 245.65	2119.97< 992.05 < 464.23

in the global variation of mycorrhizal fungal diversity and abundance. As reviewed by many authors (Kachkouch et al., 2012; Soumare et al., 2015) several factors influence arbuscular mycorrhizal fungal spores distribution, such as soil types, age of planting, cultural practices, etc. According to our results, consistent chemical drivers of AMF communities were available P, Total N, Total C, and OM soil contents. Previous studies (Nyawira et al., 2012; Edlinger et al., 2022) have shown that soil total carbon and total nitrogen contents positively influence the abundance of AMF spores. For instance, Ba et al. (2012), have reported that the allocation of C to the roots and exudation from roots to soil could

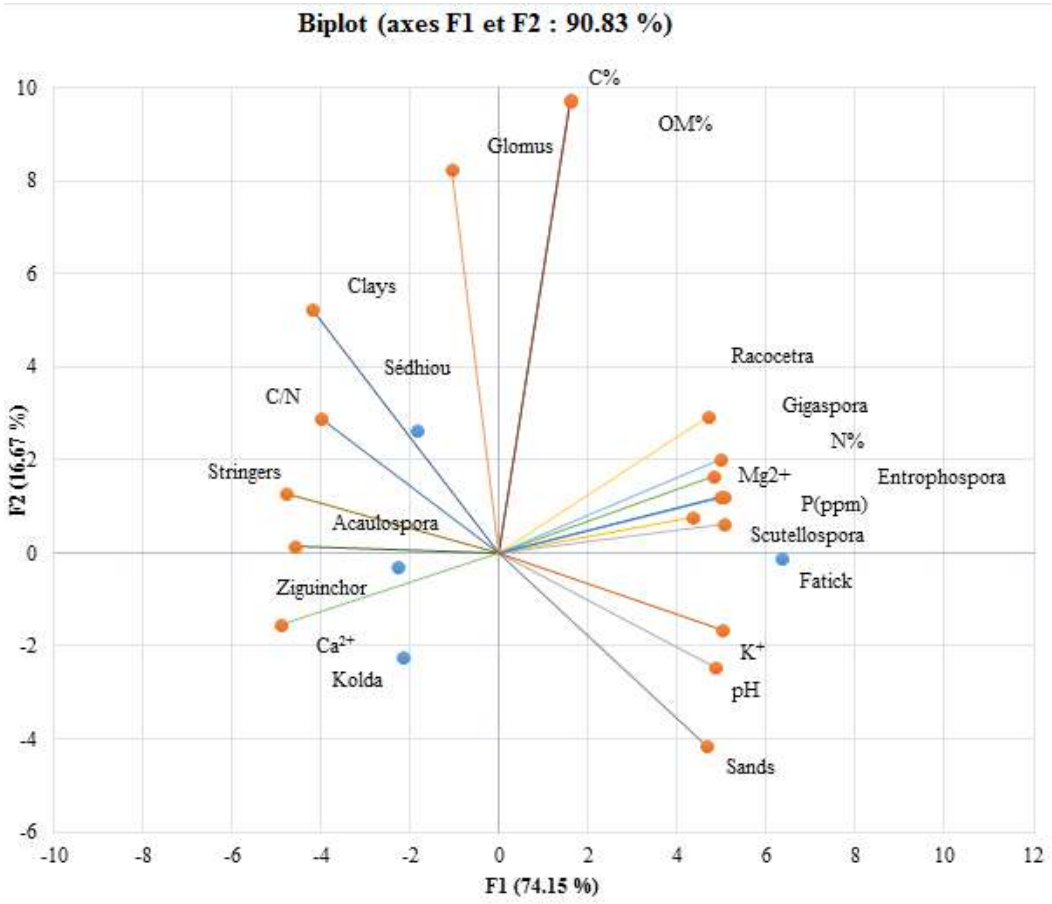

Figure 1. Principal component analysis of the diversity of arbuscular mycorrhizal fungi and physicochemical parameters of soils.

be beneficial for the sporulation of AM fungi. The present finding is in contrast to Datta and Kulkarni (2012) and Ma et al. (2023) who found negative correlation between AMF and available phosphorus. Ma et al. (2023) have shown that AMF richness and Shannon index decreased with increasing soil available P and increased with soil pH. These contradictions may be due climatic factors, and the phosphorus status of the plant.

Soil pH is another important predictor of global AMF abundance, in this study, there was an inverse relation between soil pH and spore density. This result is in line with earlier report of Cibichakravarthy et al. (2015) which have shown that pH, negatively impact on the AMF spore abundance and infective propagules. This indicates that certain AMF species are induced to sporulate abundantly under low pH as it is the case of Ziguinchor and Sedhiou in this study. In addition, soil texture and C allocation to mycorrhizae may result in low mycorrhizal fungal diversity and abundance.

In the current study, the difference in spore count and MPN, that is, high MPN versus low spore count can be explained by the fact that many AMFs, spread more with other types of propagules such as hyphae and extra-root mycelia fragments than by spores (Brito et al., 2012). The majority of spores found in soils of the present study belong to the Glomeraceae family (Driai, 2016). The dominance of the number of propagules in Kolda and Fatick could be due to the fact that in these two sites the cashew trees are associated with vegetable crops.

Regarding diversity, our study showed that spores of the genera *Glomus* and *Acaulospora* were more abundant. This result is in agreement with previous research which explains this fact by a developmental difference. Spores of *Glomus* spp. have different adaptive capacity and high plasticity to biotic and abiotic factors (Dare et al., 2013). According to Oehl et al. (2003) and Zhao et al. (2003), these genera have an outward distribution in all types of agroecosystems of the world. Fabre et al. (2021) explain this dominance by a higher spore production capacity in a shorter time compared to other genera. In addition, species of arbuscular mycorrhizal fungi belonging to the genera *Glomus* and *Acaulospora* are resistant to soil disturbances and altered ecosystems (Welemariam et al., 2018). The large

Table 4. Pearson correlation coefficients between soil chemical parameters, AMF spore abundance, and soil MPN.

Soil parameter	Sands (%)	Stringers (%)	Clays (%)	pH	P (ppm)	C (%)	N (%)	C/N	MO (%)	Ca^{2+}	Mg^{2+}	K^{+}	Total abundance	MPN of soil
Sands (%)	**1.00**													
Stringers (%)	-0.90	**1.00**												
Clays (%)	-0.97	**0.77**	**1.00**											
pH	**0.98**	-0.87	-0.96	**1.00**										
P (ppm)	**0.72**	-0.95	-0.55	**0.70**	**1.00**									
C (%)	-0.04	-0.11	**0.12**	**0.14**	**0.20**	**1.00**								
N (%)	**0.79**	-0.96	-0.64	**0.81**	**0.97**	**0.37**	**1.00**							
C/N (%)	-0.79	**0.94**	**0.65**	-0.71	-0.94	**0.14**	-0.86	**1.00**						
MO (%)	-0.04	-0.12	**0.12**	**0.15**	**0.20**	**0.99**	**0.37**	**0.14**	**1.00**					
Ca^{2+}	-0.82	**0.96**	**0.69**	-0.86	-0.94	-0.39	-1.00	**0.83**	-0.39	**1.00**				
Mg^{2+}	**0.87**	-0.86	-0.80	**0.94**	**0.76**	**0.46**	**0.90**	-0.65	**0.46**	-0.93	**1.00**			
K^{+}	**0.96**	-0.97	-0.88	**0.97**	**0.86**	**0.15**	**0.93**	-0.85	**0.16**	-0.95	**0.94**	**1.00**		
Total abundance	-0.45	**0.01**	**0.63**	-0.40	**0.28**	**0.50**	**0.19**	-0.05	**0.50**	-0.12	-0.13	-0.19	**1.00**	
MPN of soil	**0.71**	-0.35	-0.84	**0.75**	**0.06**	**0.00**	**0.25**	-0.13	**0.00**	-0.33	**0.61**	**0.56**	-0.83	**1.00**

Values in bold are significant at the threshold p-value= 0.05.

variations in AMF abundance and frequency between sites could also be due to deferential survival strategies depending on soil properties. According to Datta and Kulkarni (2012), fluctuations in the number of spores could be associated with the process of germination, formation, and degradation of spores.

Conclusion

In the present study, we have investigated the MPN, AMF spore density and diversity in soils of different *A. occidentale* L. plantations in Senegal. From the results obtained, it appeared that soil physical and chemical properties affect AMF diversity and abundance. Six AMF morphotypes belonging to *Glomus*, *Gigaspora*, *Acaulospora*, *Scutellospora*, *Entrophospora* and *Racocetra* were found. *Glomus* and *Acaulospora* genera were the predominant in all soil samples. These findings could be a starting point for the development of well performing and inocula suitable for the application in field. In future study, we will highlight if the distribution patterns differ between diversity and abundance of AMF.

CONFLICT OF INTERESTS

The authors have not declared any conflict of interests.

ACKNOWLEDGEMENTS

The authors wish to thank the project FIRST from the Government of SENEGAL for funding the work and The Joint Soil Microbiology Laboratory of Senegal for hosting this work.

REFERENCES

Agence Nationale de la Statistique et de la Démographie (ANSD) (2013). Rapport définitif RGPHAE-2013 (Recensement Général). https://ireda.ceped.org/inventaire/ressources/sen-2013-rec-o1_rapport-definitif.pdf

Agence Sénégalaise de Promotion des Exportations (ASEPEX) IRD (Institut de Recherche pour le Développement) (2017). La noix de cajou ou anacarde. Sénégal Export. https://www.senegal-export.com/produits-et-services/fruits-et-legumes/l-anacarde.html.

Aubert G (1978). Méthodes d'analyses du sol, 2nd (edà. C.N.D.P. Marseille.

Ba L, Ning J, Wang D, Facelli E, Facelli JM, Yang Y, Zhang L (2012). The relationship between the diversity of arbuscular mycorrhizal fungi and grazing in a meadow steppe. Plant Soil 352:143-156.

Barrow CJ (2012). Biochar: Potential for countering land degradation and for improving agriculture. Applied Geography 34:21-28.

Bremner JM, Mulvaney CS (1982). Nitrogen-Total. In: Methods of soil analysis. Part 2. Chemical and microbiological properties. American Society of Agronomy, Soil Science Society of America, Madison, Wisconsin.

Brito I, Goss MJ, de Carvalho M, Chatagnier O, van Tuinen D (2012). Impact of tillage system on arbuscular mycorrhiza fungal communities in the soil under Mediterranean conditions. Soil Tillage Research 121:63-67.

Camara B (2018). Caractérisation agro-écologique et socioéconomique des parcs à Elaeis guineensis Jacq. Et Faidherbia albida (Del.) Chev. et leurs influences sur la productivité du riz pluvial en Basse Casamance (Sénégal). Thèse de doctorat : Université Assane Seck de Ziguinchor, (Sénégal).

Cibichakravarthy B, Kumutha K, Balachandar D (2015). Arbuscular mycorrhizal fungal diversity in phosphorus-deficient Alfisols of a dry North-western agro-ecosystem of Tamil Nadu, India. Annals of Microbiology 65:143-153.

Cius A (2017). Appréciation du potentiel mycorhizien des sols d'arboriculture fruitière et de cultures sarclées d'Haïti par l'isolement de souches indigènes de champignons mycorhiziens arbusculaires. (Mémoire de fin d'étude). Université d'Etat d'Haïti.

Dare MO, Abaidoo R, Fagbola O, Asiedu R (2013). Diversity of arbuscular mycorrhizal fungi in soils of yam (*Dioscorea spp*.) cropping systems in four agroecologies of Nigeria. Archives of Agronomy and Soil Science 59:521-531.

Datta P, Kulkarni M (2012). Arbuscular mycorrhizal fungal diversity in sugarcane rhizosphere in relation with soil properties. Notulae Scientia Biologicae 4:66-74.

David D (1960). La détermination du sodium, du potassium, du calcium et du magnésium échangeables dans les sols par spectrophotométrie d'absorption atomique - Analyste (RSC Publishing). Division of Plant Industry 5 p.

Driai S (2016). Impact des polluants d'origine industrielle sur le développement des champignons mycorhiziens à arbuscules, sur leur diversité et sur la viabilité microbienne des sols des agro-écosystèmes du Nord-est algérien. Université Badji Mokhtar-Annaba.

Edlinger A, Garland G, Hartman K, Banerjee S, Degrune F, García-Palacios P, Hallin S, Valzano-Held A., Herzog C, Jansa J, Kost E, Maestre FT, Pescador DS, Philippot L, Rillig MC, Romdhane S, Saghaï A, Spor A, Frossard E, van der Heijden MGA (2022). Agricultural management and pesticide use reduce the functioning of beneficial plant symbionts. Nature Ecology and Evolution 6:1145-1154.

Fabre F, Burie J, Ducrot A, Lion S, Richard Q, Djidjou-Demasse R (2021). An epi-evolutionary model for predicting the adaptation of spore-producing pathogens to quantitative resistance in heterogeneous environments. Evolutionary Applications 15: 95-110.

Fisher RA, Yates F (1963). Statistical tables for biological, agricultural and medical research, edited by Fisher RA, Yates F 6th ed., 6th ed. Edinburgh: Oliver and Boyd.

Gerdemann JW, Nicolson TH (1963). Spores of mycorrhizal Endogone species extracted from soil by wet sieving and decanting. Transactions of the British Mycological Society 46:235-244. https://doi.org/10.1016/S0007-1536 (63) 80079-0.

Gianinazzi S, Vosátka M (2004). Inoculum of arbuscular mycorrhizal fungi for production systems: science meets business. Canadian Journal of Botany 82:1264-1271.

Hien S (2019). Aperçu de l'évolution de la production d'anacarde et évolution du marché de noix brutes de cajou dans la sous-région et perspectives pour 2019/2020. InForum sur le cajou sahélien 16 p.

Kachkouch W, Touhami AO, Filali-Maltouf A, Modafar CE, Moukhli A, Oukabli A, Douira A (2012). Arbuscular mycorrhizal fungi species associated with rhizosphere of *Olea europaea* L. in Morocco. Journal of Animal and Plant Sciences 15:13.

Ma X, Xu X, Geng Q, Luo Y, Ju C, Li Q, Zhou Y (2023). Global arbuscular mycorrhizal fungal diversity and abundance decreases with soil available phosphorus. Global Ecology and Biogeography 32(8):1423-1434.

Manga AGB, Ndiaye M, Ndiaye MAF, Sané S, Diop TA, Diatta AA, Bassene C, Min D, Battaglia M, Harrison MT (2022). Arbuscular Mycorrhizal Fungi Improve Growth and Phosphate Nutrition of *Acacia seyal* (Delile) under Saline Conditions. Soil System 6:79.

Mosse B (1986). Mycorrhiza in a Sustainable Agriculture. Biological Agriculture and Horticulture 3:191-209.

Ndiaye S, Charahabil MM, Diatta M (2017). Caractérisation des Plantations à base d'anacardier (*Anacardium occidentale* L.) dans le Balantacounda: cas des communes de Kaour, Goudomp et Djibanar (Casamance/Sénégal). European Scientific Journal 13:242.

Nyawira MM, Karanja D, Mwangi Wambugu G, Mwangi Mutahi J, Masiga CW, Mugoya C, Muchai M (2012). Land use practices and their implications on soil macro-fauna in Maasai Mara ecosystem. International Journal of Biodiversity and Conservation 3:15.

Oehl F, Sieverding E, Mäder P, Boller T, Wiemken A (2003). Impact of Land Use Intensity on the Species Diversity of Arbuscular Mycorrhizal Fungi in Agroecosystems of Central Europe. Applied and Environmental Microbiology 69:2816-2824.

Phillips JM, Hayman DS (1970). Improved procedures for clearing roots and stainning parasitic and vesicular-arbuscular mycorrhizal fungi for rapid assessment of infection. Transactions of the British Mycological Society 1:7.

Redecker D, Schüssler A, Stockinger H, Stürmer SL, Morton JB, Walker C (2013). An evidence-based consensus for the classification of arbuscular mycorrhizal fungi (Glomeromycota). Mycorrhiza 23:515-531.

Sadhana B (2014). Arbuscular Mycorrhizal Fungi (AMF) as a biofertilizer-a review. International Journal of Current Microbiology and Applied Sciences 3:384-400.

Samb CO, Touré M, Faye E, Ba HS, Diallo AM, Badiane S, Sanogo D (2018a). Caractéristiques sociodémographique, structurale et agronomique des plantations d'anacardier (*Anacardium occidentale* L.) du Bassin arachidier et de la Casamance / Sénégal. Journal of Animal and Plant Sciences 38:6307-6325.

Samb CO, Touré MA, Faye E, Diallo AM, Badiane S, Sanogo D (2018b). Caractéristiques sociodémographique, structurale et agronomique des plantations d'anacardier (*Anacardium occidentale* L.) du Bassin arachidier et de la Casamance/Sénégal. Journal of Animal and Plant Sciences 38(3):6307-6325.

Soumare A, Diop T, Manga AGB, Ndoye I (2015). Role of arbuscular mycorrhizal fungi and nitrogen fixing bacteria on legume growth under various environmental stresses. International Journal of Biosciences 7:31-46.

Soumare A, Sarr D, Diedhiou A (2023). Potassium sources, microorganisms, and plant nutrition—challenges and future research directions: A review. Pedosphere 33:105-115.

Souza T (2015). Handbook of Arbuscular Mycorrhizal Fungi, 1st ed. Springer International Publishing, Cham. https://doi.org/10.1007/978-3-319-24850-9

Welemariam M, Kebede F, Bedadi B, Birhane E (2018). Effect of community-based soil and water conservation practices on arbuscular mycorrhizal fungi types, spore densities, root colonization, and soil nutrients in the northern highlands of Ethiopia. Chemical and Biological Technologies in Agriculture 5:9. https://doi.org/10.1186/s40538-018-0121-4

Zhao Z, Wang G, Yang L (2003). Biodiversity of arbuscular mycorrhizal fungi in a tropical rainforest of Xishuangbanna, southwest China. Fungal Diversity 13:233-242.

Related Journals: